4364–4380 *Nucleic Acids Research, 2008, Vol. 36, No. 13* *Published online 27 June 2008*
doi:10.1093/nar/gkn384

Mrd1p binds to pre-rRNA early during transcription independent of U3 snoRNA and is required for compaction of the pre-rRNA into small subunit processomes

Åsa Segerstolpe[1], Pär Lundkvist[1], Yvonne N. Osheim[2], Ann L. Beyer[2] and Lars Wieslander[1,*]

[1]Department of Molecular Biology and Functional Genomics, Stockholm University, SE-106 91, Stockholm, Sweden and [2]Department of Microbiology, University of Virginia Health System, Charlottesville, VA 22908, USA

Received March 7, 2008; Revised May 7, 2008; Accepted May 30, 2008

ABSTRACT

In *Saccharomyces cerevisiae*, synthesis of the small ribosomal subunit requires assembly of the 35S pre-rRNA into a 90S preribosomal complex. SnoRNAs, including U3 snoRNA, and many *trans*-acting proteins are required for the ordered assembly and function of the 90S preribosomal complex. Here, we show that the conserved protein Mrd1p binds to the pre-rRNA early during transcription and is required for compaction of the pre-18S rRNA into SSU processome particles. We have exploited the fact that an Mrd1p-GFP fusion protein is incorporated into the 90S preribosomal complex, where it acts as a partial loss-of-function mutation. When associated with the pre-rRNA, Mrd1p-GFP functionally interacts with the essential Pwp2, Mpp10 and U3 snoRNP subcomplexes that are functionally interconnected in the 90S preribosomal complex. The fusion protein can partially support 90S preribosome-mediated cleavages at the A_0–A_2 sites. At the same time, on a substantial fraction of transcripts, the composition and/or structure of the 90S preribosomal complex is perturbed by the fusion protein in such a way that cleavage of the 35S pre-rRNA is either blocked or shifted to aberrant sites. These results show that Mrd1p is required for establishing productive structures within the 90S preribosomal complex.

INTRODUCTION

The biogenesis of ribosomes is largely conserved in eukaryotes and it is most extensively studied in yeast (1). In the nucleolus, RNA polymerase I produces large precursor rRNAs, the 35S pre-rRNAs that contain three of the four rRNAs, 18S, 5.8S and 25S rRNA. The fourth rRNA, 5S rRNA, is produced by RNA polymerase III. Approximately 180 *trans*-acting proteins and many small nucleolar RNAs (snoRNAs) are needed to chemically modify specific positions in the 35S pre-rRNA, cleave and fold the pre-rRNA and assemble the rRNAs with ribosomal proteins into the two ribosomal subunits, 18S rRNA in the small 40S subunit and 5.8S and 25S rRNA together with the 5S rRNA in the large, 60S subunit.

The polycistronic 35S pre-rRNA cotranscriptionally assembles into a large, approximately 90S preribosomal RNA–protein complex (2,3). Preribosomal complexes have been visualized in the electron microscopy (EM) as large terminal knobs on the growing 35S pre-rRNA during transcription. These knobs are formed as small structures that condense into larger knobs containing the entire 18S part of the 35S pre-rRNA (4). Preribosomal complexes, called small subunit (SSU) processomes (5) or 90S preribosomes (6) have also been biochemically purified. The 90S preribosomal complexes include U3 snoRNA, at least 40 *trans*-acting factors involved in the biogenesis of the small ribosomal subunit and a number of the small ribosomal subunit proteins (5–7). In addition, a number of components that are required for small subunit biogenesis, including U14, snR10 and snR30 snoRNAs (1), do not biochemically copurify with the 90S preribosomal complex, presumably due to transient or less stable associations (8–10). Most factors involved in 60S subunit biogenesis appear to associate with the pre-rRNA at a later stage, soon after the pre-rRNA is cleaved to separate the pre-40S from the pre-60S subunit (11).

In the preribosomal complexes, the 35S pre-rRNA is extensively chemically modified, including 2′-*O*-methylation of sugar moieties and pseudouridinylation of uridines (12). The modifying enzymes are guided to correct positions by different snoRNAs. A series of endo- and

*To whom correspondence should be addressed. Tel: +46 8 161720; Fax: +46 8 166488; Email: lars.wieslander@molbio.su.se

© 2008 The Author(s)
This is an Open Access article distributed under the terms of the Creative Commons Attribution Non-Commercial License (http://creativecommons.org/licenses/by-nc/2.0/uk/) which permits unrestricted non-commercial use, distribution, and reproduction in any medium, provided the original work is properly cited.

exo-nucleolytic cleavages take place. Three early cleavages, A_0 and A_1 in the 5′ external-transcribed spacer (ETS) and A_2 in the first internal transcribed spacer (ITS1) liberate a 20S pre-rRNA contained in a 43S RNP complex. This complex contains Nob1p (13,14) which, after export to the cytoplasm, is required for cleavage of the 20S pre-rRNA at site D to result in the mature 18S rRNA.

Biochemical analyses have suggested that in many species processing of the 35S pre-rRNA in the 90S preribosomal complex, including chemical modifications and A_0–A_2 cleavage, is posttranscriptional (15). However, cleavage at A_0 has been reported to occur cotranscriptionally in *Saccharomyces cerevisiae* (16). EM studies in *Dictyostelium* and in exponentially growing yeast have shown that the 35S pre-rRNA can also be cotranscriptionally cleaved at A_2, probably after chemical modifications have been introduced (4,17). Regardless, if cleavages at A_0–A_2 occur cotranscriptionally or posttranscriptionally, the folding of the 35S pre-rRNA must be highly coordinated to allow the different processing steps to occur in a timely order and presumably before the compact structure of the ribosomal subunits form. In the 90S preribosomal complex, several subcomplexes have been identified (18,19). The U3 snoRNP has a central role. The Pwp2 complex, probably identical to the UTP-B complex (18,20), and the Mpp10/Imp3/Imp4 complex (21) are important for U3 snoRNP binding to the 35S pre-rRNA. The subcomplex consisting of the transcription-Utps (t-Utps), which is similar to the UTP-A subcomplex, associates with the ribosomal chromatin and with the 35S pre-rRNA independently of U3 snoRNP (22) and is needed for efficient transcription by RNA polymerase I. Utp22p, a component of the stable UTP-C complex (18), has been found in the 90S preribosomal complex. As is the case for Rrp7p, which is also part of the UTP-C complex, Utp22p is required for synthesis of 18S rRNA (7,23). These components are also present in a complex similar to UTP-C that appears to be involved in coupling transcription of ribosomal protein genes and pre-rRNA processing (24).

It is intriguing that so many different *trans*-acting factors are needed to ensure that the A_0–A_2 cleavages take place. Cleavage at A_0 is not essential for cell viability. The A_0 cleavage requires that the U3 snoRNA base pairs to a sequence located 140-nt upstream of the A_0 site in the 5′ ETS (25–27). Other factors influence cleavage at A_0 and as a rule cleavage at A_0 is coupled to cleavage at A_1–A_2. Cleavage at A_1 and A_2 are even more closely coupled, and recognition of these cleavage sites in both cases involves a conserved nucleotide sequence and a fixed distance from a stem–loop structure in the 35S pre-rRNA. U3 snoRNA has a central role in the A_0–A_2 cleavages and interacts with the 35S pre-rRNA in a complex manner. Apart from the base pairing upstream of the A_0 site, U3 snoRNA base pairs at the 5′-end of the 18S rRNA and to a sequence within the 18S rRNA, two regions that are involved in formation of the pseudoknot present in the mature 18S rRNA (28–30). This base pairing blocks the formation of the pseudoknot and may be a way of both preventing premature folding and guiding correct folding.

To understand ribosome biogenesis, it is important to know how the dynamic structure of the 35S pre-rRNA is formed in a coordinated manner within the 90S preribosomal complex. It is likely that the 90S preribosomal complex coordinates pre-rRNA folding and regulates accessibility of factors interacting with the 35S pre-rRNA (1,31). The 90S preribosomal complex may perform this function as a unit. A more dynamic model is that individual subcomplexes, including snoRNPs, influence the structure of the pre-rRNA, possibly resulting in a succession of structures needed to achieve quality control (19). The cleavage mechanisms and the function of most of the individual *trans*-acting factors in the 90S preribosomal complex are so far unknown. In addition, it is not known how a correct and controlled folding of the pre-rRNA is achieved.

We have previously identified a protein, Mrd1p (32), that is essential for cleavages at sites A_0–A_2. Mrd1p can be coimmunoprecipitated with 35S pre-rRNA, but has not been identified as a stable component of the biochemically purified U3 snoRNA-containing preribosomal complexes. A prominent feature of Mrd1p is the presence of five RNA-binding domains (RBDs) that are conserved as to position and sequence (33). This structure of Mrd1p distinguishes it from the majority of 90S complex proteins, which contain no recognizable RNA-binding motifs, and makes it an attractive candidate to play a role as a pre-rRNA chaperone. Additionally, Mrd1p is one of only three RBD-containing proteins that are conserved throughout eukaryotic evolution (34).

Here, we report the analyses of the defects in preribosomal processing induced by depletion of Mrd1p or by the presence of a mutant Mrd1p. This extends our knowledge about the structural and functional connection between Mrd1p and the preribosomal complex. We show that Mrd1p interacts early with pre-rRNA, independent of U3 snoRNP and key Utps, and that Mrd1p is required for compaction of the pre-rRNA into SSU processomes. We further show that a mutant Mrd1 allele, in addition to causing a general defect in ribosomal (18S) biogenesis, both disturbs U3 snoRNP association with pre-rRNA and drastically increases synthesis of an aberrant rRNA product, the 22.5S rRNA. The 22.5S rRNA is made in the nucleus by a premature cotranscriptional cleavage event and in the context of a 90S preribosomal complex. We finally establish that the growth and aberrant processing of the mutant is sensitive to changes in processome composition. This indicates that Mrd1p functionally interacts with specific 90S preribosomal complex components and is essential for formation of structures within the 90S preribosomal complex productive for cleavages at A_0–A_2.

MATERIALS AND METHODS

Yeast strains, plasmids and genetic manipulations

Conditional mutant, epitope-tagged and deletion strains were generated by a one-step PCR strategy (35) via homologous recombination. The epitope-tagged versions of the genes were expressed from their endogenous promoters and in each case were the sole source of the protein

Table 1. *Saccharomyces cerevisiae* strains used in this study

Isogenic derivates of AA255	
PLY023	*MATa ura3-52 leu2-3,112 HIS3 lys2Δ201 ADE2 mrd1-13Myc-kanMX6*
PLY094	*MATa ura3-52 leu2-3,112 his3Δ200 lys2Δ201 ADE2 GAL2*
PLY129	*MATa ura3-52 leu2-3,112 his3Δ200 lys2Δ201 ADE2 GAL2 mrd1-GFP-kanMX6*
PLY172	*MATa ura3-52 leu2-3,112 his3Δ200 lys2Δ201 ADE2 GAL2 hisMX6-PGAL1-3HA-nop58 mrd1-GFP-kanMX6*
PLY178	*MATα ura3-52 leu2-3,112 his3Δ200 lys2Δ201 ADE2 GAL2 hisMX6-PGAL1-3HA-mrd1*
PLY255	*MATa ura3-52 leu2-3,112 his3Δ200 lys2Δ201 ADE2 GAL2 rpa12 :: LEU2 mrd1-GFP-kanMX6*
PLY339	*MATα ura3-52 leu2-3,112 his3Δ200 lys2Δ201 ADE2 GAL2 hisMX6-PGAL1-3HA-mpp10 mrd1-GFP-kanMX6*
PLY340	*MATα ura3-52 leu2-3,112 his3Δ200 lys2Δ201 ADE2 GAL2 hisMX6-PGAL1-3HA-pwp2 mrd1-GFP-kanMX6*
PLY341	*MATa ura3-52 leu2-3,112 his3Δ200 lys2Δ201 ADE2 GAL2 hisMX6-PGAL1-3HA-utp4 mrd1-GFP-kanMX6*
PLY342	*MATα ura3-52 leu2-3,112 his3Δ200 lys2Δ201 ADE2 GAL2 hisMX6-PGAL1-3HA-nob1*
PLY344	*MATa ura3-52 leu2-3,112 his3Δ200 lys2Δ201 ade2 GAL2 hisMX6-PGAL1-3HA-nob1 mrd1-GFP-kanMX6*
PLY391	*MATa/α ura3-52/ura3-52 leu2-3,112/leu2-3,112 his3Δ200/his3Δ200 lys2Δ201/lys2Δ201 hisMX6-PGAL1- 3HA-pwp2/PWP2 mrd1-GFP-kanMX6/MRD1*
PLY392	*MATa ura3-52 leu2-3,112 his3Δ200 lys2Δ201 ADE2 GAL2 rpa12 :: LEU2 utp13-GFP-kanMX6*
PLY397	*MATa ura3-52 leu2-3,112 his3Δ200 lys2Δ201 ADE2 GAL2 mrd1-ProtA-klURA3*

in the cell. The hisMX6-GAL1-3HA cassette was inserted via homologous recombination in frame and just upstream of the gene in the genome to obtain the conditional mutant strains. PLY129 was crossed with the conditionally mutant strains and sporulated to yield the PLY172, 339, 340, 341 and 344 strains. These strains are referred to in the text as *GAL::3HA-NOP58/MRD1-GFP, GAL::3HA-MPP10/MRD1-GFP*, *GAL::3HA-PWP2/MRD1-GFP, GAL::3HA-UTP4/MRD1-GFP* and *GAL::3HA-NOB1/MRD1-GFP*, respectively. The genotypes of the strains used in this study are listed in Table 1.

Yeast strains were transformed using the lithium acetate method (36) and the correct integration and expression was verified by PCR and western blot analysis.

The plasmids pUN100-DsRed-Nop1 and pEG-KT/Mrd1 were transformed into PLY129 and PLY094, respectively, using the lazy-bone transformation procedure (37).

Northern blot analysis

RNA was separated on 1% agarose–formaldehyde gels as described (38) and blotted onto a Zeta-probe membrane (BioRad, Hercules, California, USA) and UV cross-linked. The following oligonucleotide probes were used: probe 1 (5′-GGTCTCTCTGCTGCCGG-3′), probe 2 (5′-GCTCTCATGCTCTTGCC-3′), probe 3 (5′-GCCACTA TCCTACCATCG-3′), probe 4 (5′-ACTCGCCGTTACT AAGGC-3′), U3 snoRNA probe (5′-TAGATTCAAT TTCGGTTT-3′), U14 snoRNA (5′-TCACTCAGACAT CCTAGG-3′). Oligonucleotide probes were end-labelled with T4 polynucleotide kinase (New England Biolabs, Ipswich, Massachusetts, USA) and (g-^{32}P) ATP (Perkin Elmer, Waltham, Massachusetts USA) and purified using the Qiaquick Nucleotide Removal Kit (Qiagen). Prehybridization and hybridization were performed in 5× SSPE (1× SSPE is 150 mM NaCl, 10 mM Na_2HPO_4 H_2O, 1 mM EDTA, pH 7.4), containing 7% SDS, 1× Denhardt solution and 100 mg/ml salmon sperm DNA, at a temperature of *T*m—9°C. The filters were washed in 3× SSPE, 0.5% SDS, 5× Denhardt solution at hybridization temperature and in 1× SSPE, 0.1% SDS at 37°C. Intensities of the pre-rRNA and rRNA bands were analyzed with a phosphoimager (Fuji, FLA3000) and quantified with Fuji Multi Gauge V3.0 software.

Chromatin (Miller) spreads

Miller spreads were made as described (4). Briefly, cells were grown to OD_{600} = 0.4–0.6 at 30°C. One milliliter of culture was digested with prewarmed 5 mg zymolyase dissolved in 200 ml of growth medium. After 4 min digestion at 30°C, cells were spun down for 10 s and the pellet was resuspended in 1 ml of 0.025% Triton X100 (pH 9.0). This suspension was immediately diluted into 6 ml of 11 mM KCl (pH 8.0) and allowed to disperse for 20 min. One-tenth volume of 0.1 M sucrose-10% formalin (pH 8.7) was added, and the chromatin was deposited on EM grids by centrifugation through a cushion of the sucrose–formalin solution.

Ribonuclease protection

Labeled single-stranded RNA probe was prepared by *in vitro* transcription of a PCR fragment using a-^{32}P UTP and T7 RNA polymerase. The labelled RNA was purified by gel electrophoresis using a 4% sequencing gel. The probe was hybridized to RNA extracted from isolated yeast cell nuclei or from yeast cells, treated with RNase A and RNase T1 and analyzed by gel electrophoresis essentially as described (38).

Immunoprecipitation

Extracts from 20 OD_{600} units of exponentially growing cells ($OD_{600} \sim 0.5$ nm). were lyzed with glass beads in IP buffer, consisting of 10 mM Tris–HCl (pH 7.5), 5 mM $MgCl_2$, 150 mM NaCl, 0.1% SDS, containing complete protease inhibitor (Roche Applied Science, Basel, Switzerland), 20 mM Ribonucleoside Vanadyl Complexes (Sigma, St. Louis, Missouri, USA) and 100 U RNaseOUT (Ambion, Austin, Texas, USA). The supernatant was incubated with polyclonal anti-GFP antibodies (BD Living Colours) for 2 h at 4°C. GammaBind G Sepharose beads (Amersham Biotechnology, Piscataway, New Jersey, USA) were precoated with 100 mg/ml tRNA and 100 mg/ml BSA and incubated with the extract

for 1 h at 4°C. Immunoprecipitates were washed for 5 min twice with IP buffer containing 10 mM Ribonucleoside Vanadyl Complexes and three times with IP buffer lacking the Ribonucleoside Vanadyl Complexes. RNA was extracted with 400 ml buffer (50 mM sodium acetate (pH 5.2), 10 mM EDTA, 1% SDS), followed by phenol/chloroform purification and ethanol precipitation. RNA was analyzed by northern blot and hybridized as described above.

Isolation of yeast nuclei

Pure yeast cell nuclei were isolated as described previously (39).

Sucrose gradient analysis

A total of 200 ml of exponentially growing yeast cells were incubated with 0.1 mg/ml cycloheximide (Sigma, St. Louis, Missouri, USA) for 10 min at 30°C. The cells were washed in ddH_20, lyzed with glass beads and resuspended in 3 ml lysis buffer [20 mM HEPES (pH 7.5), 10 mM KCl, 2.5 mM $MgCl_2$, 1 mM EGTA (pH 8), 0.1 mg/ml cycloheximide, 1 mM DTT]. The extract was centrifuged in a microcentrifuge at 15 000*g* for 10 min at 4°C and 100 $OD_{260\,nm}$ units of the supernatant were layered onto 10–50% sucrose gradients, which had been prepared in lysis buffer without cycloheximide and DTT. Ultracentrifugation was performed in a SW40 rotor (Beckman) at 39 500 r.p.m. for 155 min at 4°C. Fractions of 500 ml were collected. One half of that was trichloroacetic acid precipitated and analyzed by western blot. The other half was analyzed by northern blot. Positions of 40S and 60S subunits and 80S ribosomes in the gradients were determined from the positions of 18S and 25S rRNA.

RT–PCR

Analysis of circularized RNA. RNA was extracted with the hot-phenol method (40) from 20 OD_{600} units of cells. A total of 5 mg of RNA was self-ligated with T4 RNA ligase (New England Biolabs) in a volume of 10 ml containing T4 ligase buffer from the manufacturer and 1 ml DMSO overnight at 16°C. After heating at 65°C for 5 min, the reaction was adjusted to a volume of 100 ml, phenol/chloroform extracted and precipitated with ethanol. The RNA was dissolved in 10 ml ddH2O and first strand synthesis carried out with primer Ci-RT (5′-CACAGTCTTGCGACCGGC-3′) using Transcriptor reverse transcriptase (Roche Applied Science) following the instructions in the manual. cDNA fragments of the 5′-3′ end-ligated rRNA were amplified with primer pairs Ci-RT and Ci-18S 3′ (5′-AACTCCATCTCAGAGCGG AG-3′) followed by a nested PCR with primer pairs Ci-18S 3′ and Ci-ETS 5′ (5′-TCCTTCGCTGCTCA CCAATG-3′) using 1 ml of the amplification products from the first PCR as the template. The products were gel purified, ligated into pGEM T easy vector (Promega, Madison, Wisconsin, USA) and used to transform JM109. Sequence analysis was performed on 54 different clones (MWG-Biotech AG, Ebersberg, Germany).

Analysis of mRNA. RNA was extracted as above from 20 $OD_{600\,nm}$ units of cells from the PLY129, PLY339 and PLY340 strains. Aliquots were treated with RNAse-free DNase I for 20 min at 37°C and purified by phenol extraction. Four micrograms of RNA was reverse transcribed, using Superscript III Reverse Transcriptase (Invitrogen) and two specific primers, one for MRD1 and the other for MPP10 or PWP2. The cDNA was amplified with Platinum Taq DNA polymerase (Invitrogen) using 25 cycles in a reaction containing primer pairs for MRD1 and MPP10 or PWP2. ^{32}P-labeled 5′ primers were included and the PCR products were analyzed by electrophoresis in 1.7% agarose gels. The PCR products were quantified as described.

Western blot analysis

The primary antibodies used were monoclonal anti-GFP (1:5000, JL-8, Clontech, Mountain View, California, USA), monoclonal anti-Nop1p (1:2000, 38F3, Encor Biotechnology, Gainsville, Florida, USA), monoclonal anti-c-Myc (1:2000, 9E10, Santa Cruz Biotechnology, Santa Cruz, California, USA), monoclonal anti-yeast cytoplasmic vacuolar carboxypeptidase Y (CPY) (1:5000, 10A5-B5, New Biotechnology), anti-HA peroxidase monoclonal antibody (1:1000, 3F10, Roche) and polyclonal anti-Mpp10p antibodies (1:10000) (41). The polyclonal goat anti-mouse and swine anti-rabbit HRP coupled antibodies (1:1000–1:3000, DakoCytomation) were used for immunodetection with the ECL solution (Amersham Biosciences).

Fluorescence microscopy

Exponentially growing yeast cells were mounted on glass slides covered with 1% agarose. To detect Mrd1p-GFP, Utp13p-GFP and DsRED-Nop1p, epifluorescence microscopy was carried out at 100× magnification in a Zeiss Axioplan 2 fluorescence microscope (Zeiss).

RESULTS

An Mrd1p-GFP fusion protein acts as a partial loss-of-function mutation of Mrd1p

Mrd1p is not a stable component of the biochemically purified SSU processome. Even so, it is required for cleavages of the 35S pre-rRNA at the A_0, A_1 and A_2 cleavage sites (32; see Figure 1A for positions of these cleavage sites). We therefore wished to test the hypothesis that Mrd1p functionally and physically interacts with the SSU processome components in a 90S preribosomal RNP complex in the cell. While depletion of Mrd1p completely inhibits growth, fusion of a GFP coding domain to the 3′-end of the coding region of the genomic MRD1 gene resulted in an approximately 2.7 times longer generation time. No such effect was recorded when Mrd1p was C-terminally tagged with 13Myc or protein A (Figure 1B and C). The amount of 18S rRNA was considerably reduced in the presence of Mrd1–GFP, whereas the amount of 25S rRNA was not significantly affected (Figure 1D). The extent of 18S rRNA reduction was measured by hybridization with probes specific for 18S and 25S rRNA (data not shown). Quantification of the

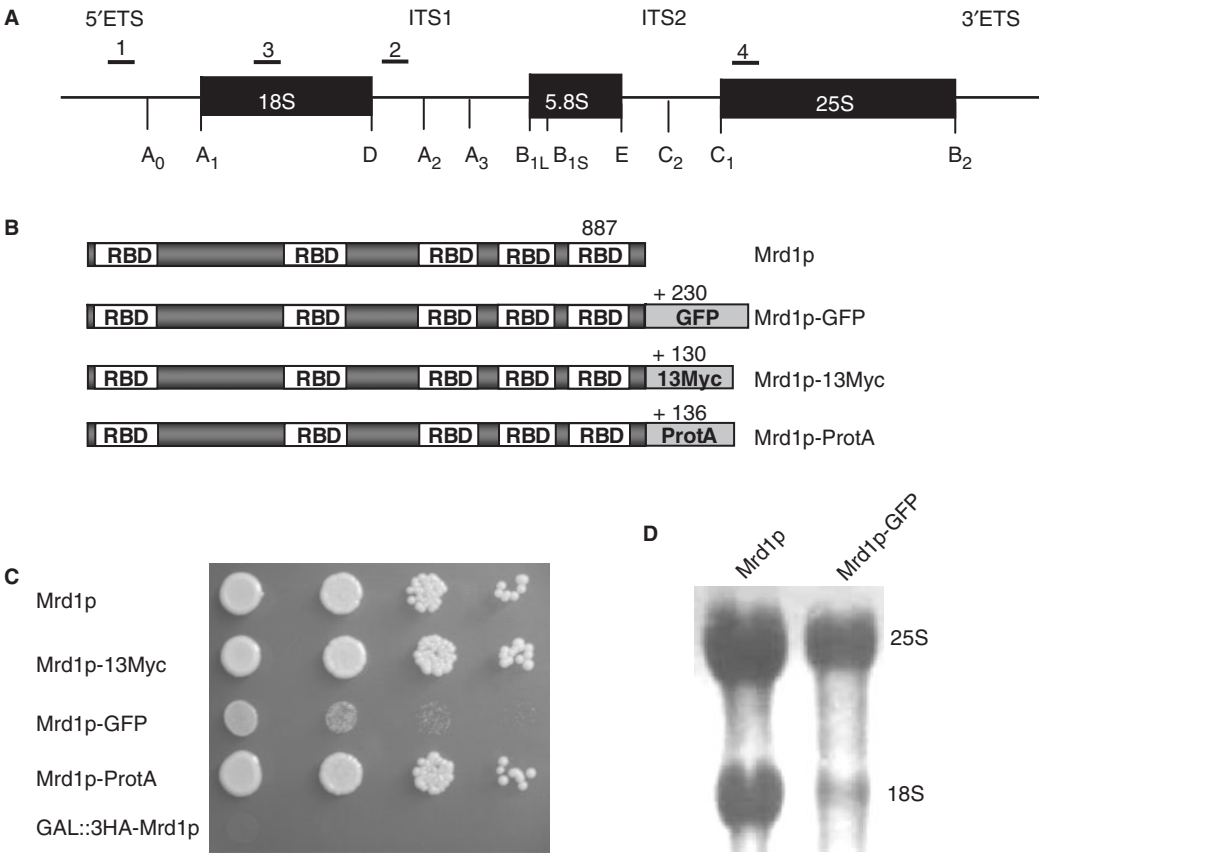

Figure 1. The Mrd1p-GFP fusion protein acts as a partial loss-of-function mutation of Mrd1p. (**A**) Schematic representation of the 35S pre-rRNA. A_0 to E represent cleavages during processing. The numbers 1–4 show the positions of the oligonucleotides used as probes in northern blot hybridizations. (**B**) Schematic representation of Mrd1p and modified versions of Mrd1p used in this study. Positions of the five RBDs in Mrd1p and the lengths of Mrd1p in amino acid residues and the different tags are shown. (**C**) Growth on YPD of strains containing Mrd1p or the different versions of Mrd1p. The doubling time was ~110 min for Mrd1p, 106 min for Mrd1p-13Myc, 300 min for Mrd1p-GFP and 100 min for Mrd1p-ProtA. Depletion of Mrd1p (GAL::3HA-Mrd1p) is not compatible with growth (bottom row). (**D**) RNA was extracted from cells containing Mrd1p or Mrd1p-GFP, subjected to electrophoresis in 1% agarose/formaldehyde gels and transferred to a membrane. The 25S and 18S rRNAs were visualized by methylene blue staining.

hybridization signals showed that the 18S/25S rRNA ratio was reduced 3–4 times, showing that the steady-state amount of 18S rRNA in the Mrd1p-GFP strain was significantly reduced, though not to the same extent as after Mrd1 depletion (32).

The effect on synthesis of 18S rRNA and growth shows that Mrd1p-GFP acts as a partial loss-of-function mutation of Mrd1p. The extra C-terminal GFP domain might alter important functional interactions of Mrd1p and analyses of the Mrd1p-GFP fusion is conceptually similar to studying defects caused by other types of mutations in essential genes. As a means to learn more about the function of Mrd1p in the biogenesis of 40S ribosomal subunits, we therefore investigated the molecular basis for the influence of the Mrd1p-GFP fusion protein on 18S rRNA synthesis and cell growth.

Mrd1p-GFP accumulates in the nucleolus and assembles with 35S pre-rRNA into 90S preribosomal complexes

The partial loss-of-function could theoretically be due to a de-localization of Mrd1p-GFP from the normal site of action caused by the GFP domain. This makes it important to establish the location of Mrd1p-GFP in the cell. Mrd1p-GFP colocalized with the nucleolar specific Nop1p in the nucleolus, where it was highly concentrated (Figure 2A). A fraction of Mrd1p-GFP was also detected in the nucleoplasm. This pattern was the same as that of Mrd1p tagged with a 3HA tag (32) or a 13Myc tag (data not shown). We then asked if the accumulation of Mrd1p-GFP in the nucleolus was dependent on RNA polymerase I transcription. We constructed a rpa12::LEU2 deletion strain with Mrd1p-GFP. Rpa12 is a subunit of RNA polymerase I that is dispensable at room temperature but becomes essential at 37°C (42). After shift to nonpermissive temperature, western blot analysis showed that the Mrd1p-GFP amount was initially reduced, within 1 h, but then remained relatively stable for several hours (Figure 2C). An initial reduction in Mrd1p-GFP signal was also seen in the microscope. Importantly, there was a redistribution of Mrd1p-GFP within the nucleus. Three hours after the shift to 37°C and even more so after 5 h, Mrd1p-GFP no longer accumulated in the nucleolus (Figure 2B). In the PLY129 strain, containing the wild-type RPA12 gene, Mrd1p-GFP remained in the nucleolus under these conditions (data not shown). Also RBD1, the Mrd1p orthologue in insect cells, is dependent on RNA

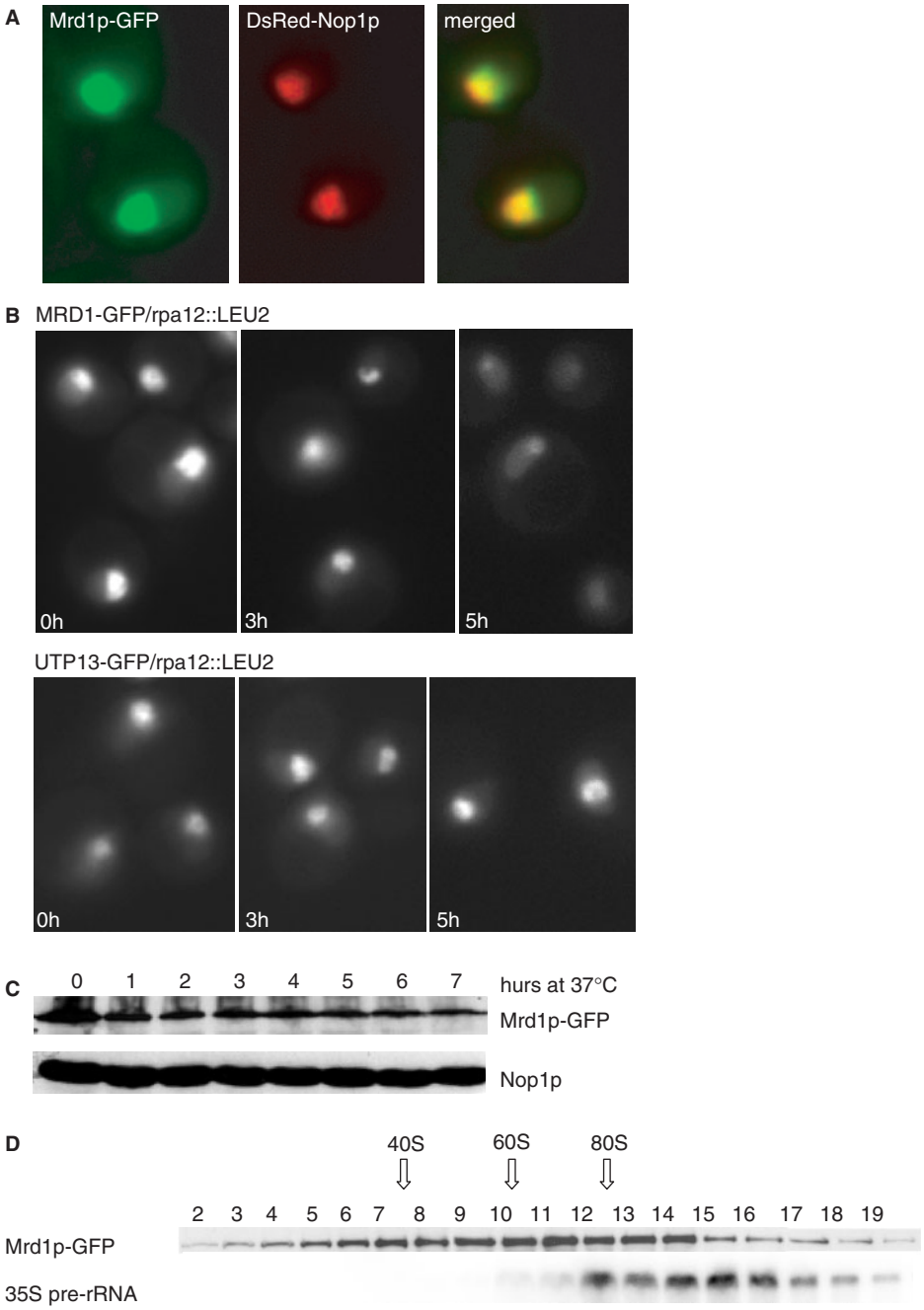

Figure 2. Mrd1p-GFP is located primarily in the nucleolus and this localization is dependent on transcription by RNA polymerase I. (**A**) Mrd1p-GFP and DsRed-Nop1p colocalized in the nucleolus. The Mrd1p-GFP strain was transformed with pUN100-DsRed-NOP1 and grown in synthetic media lacking leucine and analyzed with fluorescence microscopy. (**B**) Localization of Mrd1p-GFP and Utp13p–GFP by fluorescent microscopy after shut off of RNA polymerase I transcription. Cells containing Mrd1p-GFP or Utp13p–GFP together with a temperature sensitive RNA polymerase I allele (rpa12::LEU2) were grown at permissive temperature (0 h) and shifted to 37°C for 3 h and 5 h. (**C**) Stability of Mrd1p-GFP analyzed by western blotting. Cells containing Mrd1p-GFP and a temperature-sensitive RNA polymerase I allele (rpa12::LEU2) were grown at permissive temperature (0 h) and shifted to 37°C for 1–7 h. Nop1p acted as a loading control. (**D**) Sucrose gradient analyses of extracts from cells with Mrd1p-GFP. Mrd1p-GFP was identified by western blot analyses of each fraction. The 35S pre-rRNA was identified by northern blot analyses using probe 1. The positions of 40S, 60S and 80S are indicated, as determined from methylene blue staining of the RNA in each fraction.

polymerase I transcription for its nucleolar accumulation (33), suggesting that this is an intrinsic property of the protein and was not due to the GFP tag of Mrd1p-GFP. We also analyzed the behavior of a SSU processome component, Utp13p–GFP, upon cessation of transcription by RNA polymerase I (Figure 2B). Compared to Utp13p–GFP, Mrd1p-GFP accumulation in the nucleolus was more sensitive to transcription shut off. We conclude that the GFP domain did not displace Mrd1p-GFP from its normal, predominantly nucleolar location, and that the accumulation in the nucleolus of Mrd1p was dependent on RNA polymerase I transcription, more so than the

bona fide SSU processome component Utp13p. Utp13p is part of the stable UTP-B subcomplex (18), while Mrd1p has not been found in any stable subcomplex. This difference could influence their different localization behavior, and suggests that the nucleolar enrichment of Mrd1p is mainly dependent on the presence of newly synthesized pre-rRNA.

In accordance with this interpretation, analyses of pre-rRNA–protein complexes by sucrose gradient sedimentation showed that Mrd1p-GFP and 35S pre-rRNA were both found in the 80–90S region of the gradient (Figure 2D). This was further consistent with immunoprecipitation experiments that showed that Mrd1p-GFP could be coimmunoprecipitated with 35S pre-rRNA (Figure 6B).

We conclude that Mrd1p-GFP accumulates in the nucleolus and that a substantial amount of Mrd1p-GFP assembles into 90S preribosomal complexes together with 35S pre-rRNA. It is therefore likely that the functional defects observed in the presence of Mrd1p-GFP are introduced in the setting of the 90S preribosomal complex.

Mrd1p-GFP partially inhibits cleavage of 35S pre-rRNA at A_0–A_2 and induces processing at aberrant sites

We next asked if the Mrd1p-GFP influenced any of the A_0–A_2 cleavages of the 35S pre-rRNA. There was a substantial accumulation of 35S pre-rRNA and also of 23S rRNA (5′-end to A_3) in the presence of Mrd1p-GFP, while the level of 20S pre-rRNA (A_1–A_2) was reduced (Figure 3A). The aberrant 23S species characteristically accumulates when cleavages at A_0, A_1 and A_2 are delayed. We could not detect accumulation of 32S pre-rRNA (cleaved at A_1) (in shorter exposures). Northern blots were also hybridized with a probe complementary to a region located between cleavage sites A_2 and A_3 (data not shown). No accumulation of 21S rRNA (A_1–A_3) could be detected, showing that the pre-rRNA species in Figure 3A was 20S and not 21S and that cleavage at A_1 was not much more effective than cleavage at A_2. We also did not detect 22S rRNA (A_0–A_3), showing that cleavage at A_0 was not much more efficient than at A_1 and A_2, The steady-state levels of the pre-rRNA species detected in the northern blots were therefore consistent with the conclusion that the cleavages at A_0–A_2 were impaired in the presence of Mrd1p-GFP.

Most significantly, in addition to the accumulation of 35S pre-rRNA and 23S rRNA in Mrd1p-GFP cells, we observed the accumulation of an unusual rRNA processing product, migrating slightly faster than 23S rRNA (Figure 3B). The amount of the new processing product was almost the same as that of 23S rRNA and could only be detected in the strain with the GFP-tagged version of Mrd1p (Figure 3B, compare lane 3 with 1 and 2). It is not seen when Mrd1 is depleted (32). According to its migration, this rRNA species was ~2550-nt long. It hybridized with an oligonucleotide probe located 5′ of the A_0 cleavage site (Figure 3B, probe 1), but not with oligonucleotide probe 2, corresponding to a sequence between 39 and 56 nucleotides 3′ of the D site (Figure 3A). We therefore conclude that this new processing product extends from the 5′-end of the 35S pre-rRNA (or close to it) to a position near the D cleavage site, located not more than ~50-nt downstream of the D site. We named this aberrant processing product 22.5S rRNA.

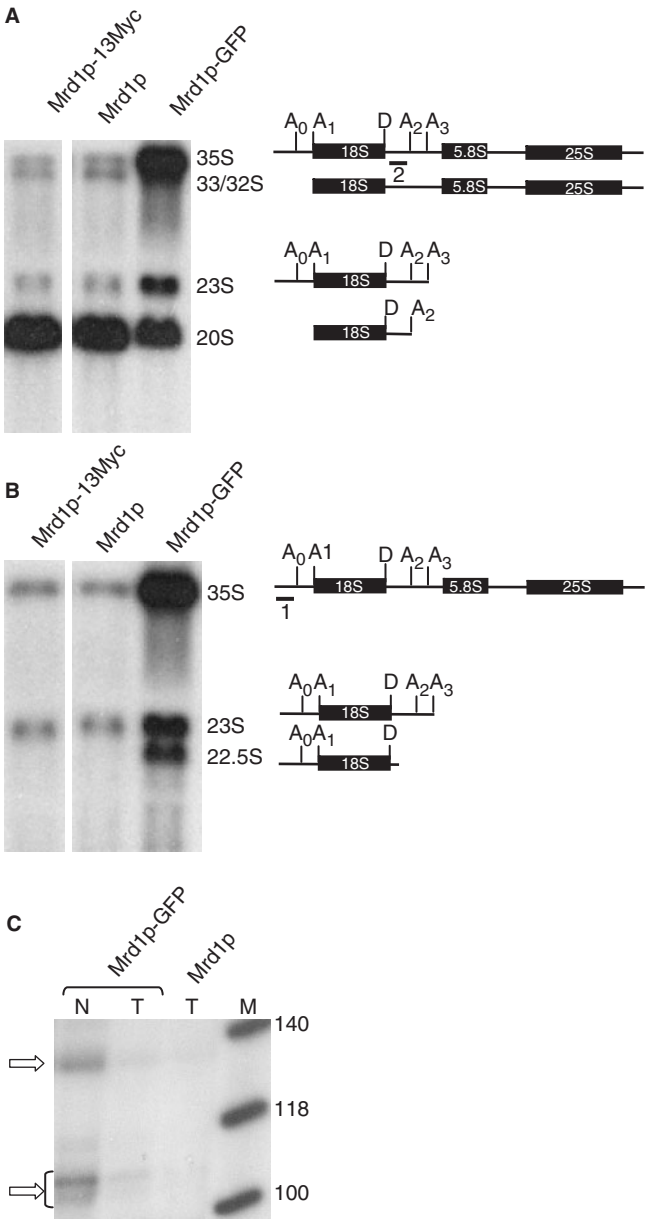

Figure 3. Mrd1p-GFP partially inhibits the A_0–A_2 cleavages and induces aberrant processing products with 3′-ends located in a narrow region just downstream of the D site. (**A** and **B**) Northern hybridizations using probes specific for pre-rRNA species. RNA was extracted from wild-type cells (Mrd1p), Mrd1p-13Myc and Mrd1p-GFP cells and separated on 1% agarose/formaldehyde gels. Schematic representations of identified pre-rRNA species and probes used are indicated to the right of each panel. Probe 2 was used in (A), and probe 1 was used in (B). (**C**) RNase protection analyses using a 164-nt long fragment covering the 18S rRNA-ITS1 border. RNA was extracted from purified nuclei and from cells expressing Mrd1p-GFP or from cells expressing Mrd1p. The probe extended from a position 100-nt upstream of the D cleavage site to a position located 64-nt downstream of the D site. Protected RNAs, indicated by arrows, were analyzed in 8% polyacrylamide/urea gels. N, nuclear RNA; T, total cellular RNA; M, size markers.

We mapped the 3′-end of 22.5S rRNA in more detail by RNAse protection, using an *in vitro* transcript extending from a position 100-nt upstream of the 3′-end of 18S rRNA (the D site) to a position 64-nt downstream of the D site (Figure 3C). We detected protected fragments corresponding to 3′-ends between 5- and 12-nt downstream of the D site and a fragment corresponding to a site about 35-nt downstream of the D site. These sites were well detected in nuclear RNA from the Mrd1p-GFP strain and they were seen in total RNA from the Mrd1p-GFP strain. We also circularized nuclear or total RNA with RNA ligase, followed by RT–PCR, cloning and sequencing of individual PCR products (data not shown). A majority of the 3′-ends detected in this assay were located between 4- and 9-nt downstream of the D site. In both the RNAse protection (Figure 3C) and the ligation–RT–PCR analyses, we detected fragments with the aberrant 3¢ ends also in wt cells, but in considerably lower amounts. Combined, the northern blots, RNAse protection and ligation experiments suggest that the 3′-end of the 22.5S rRNA is heterogeneous, with most individual molecules ending 5-to 12-nt downstream of the D cleavage site. Our results also suggest that these fragments are present in wt cells in small amounts and that the Mrd1p-GFP drastically increases the generation of the aberrant cleavages.

The generation of substantial amounts of the aberrant 3′-ends was dependent on the presence of the GFP domain at the C-terminus of Mrd1p (Figure 3B). Appearance of the 22.5S rRNA was also dependent on a minimum amount of Mrd1p-GFP. While the aberrant RNA was seen in a haploid strain and in a wt strain expressing large amounts of Mrd1p-GFP from a high copy plasmid with the GAL1 promoter, we did not see it in a diploid strain with the *MRD1-GFP*/*MRD1* genotype (data not shown).

The aberrant processing takes place in the nucleus and is not dependent on Nob1p

We wished to find out which molecular system was responsible for generating the aberrant 3′-ends 5- to 12-nt downstream of the D site. It was possible that the aberrant 3′-ends were due to Mrd1p-GFP induced events via the processome machinery in the nucleolus. It was also possible that Mrd1–GFP induced export of abnormal pre-rRNP complexes to the cytoplasm, which were subsequently abnormally processed by the machinery responsible for cleavage at the D site. We first wished to know where in the cell the 22.5S rRNA was generated. We therefore isolated pure yeast nuclei. A cytoplasmic protein marker (CPY) was not detected in the nuclear preparation (Figure 4B). Northern blot analyses showed that the 22.5S rRNA was present in the nuclei together with 35S pre-rRNA, 23S rRNA and 20S pre-rRNA (Figure 4A).

Even if the aberrant processing takes place in the nucleus, it was still possible that Nob1p could be involved. Nob1p is likely to be the endonuclease responsible for cleavage at the D site in 20S pre-rRNA in the cytoplasm. However, Nob1p is known to be associated with pre-40S ribosomal particles in the nucleus (13,14). We constructed a strain with Nob1p under the control of a galactose inducible promoter together with the *MRD1-GFP* allele. When Nob1p was efficiently depleted in glucose (Figure 4C), 20S pre-rRNA accumulated as expected (Figure 4D). In these conditions, the 22.5S rRNA processing product was still made (Figure 4E).

We conclude that the 3′-ends of the 22.5S rRNA are generated in the nucleus and are not dependent on Nob1p, and therefore most likely are not performed by the machinery responsible for cleavage at the D site.

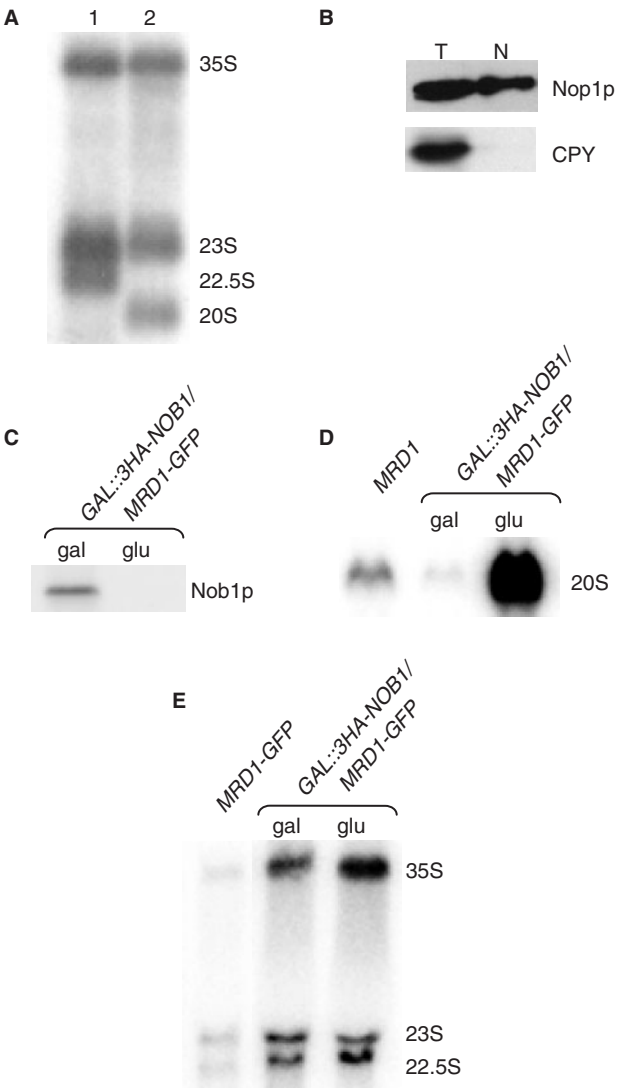

Figure 4. The aberrant cleavages producing 22.5S rRNA take place in the cell nucleus and are not dependent on Nob1p. (**A**) RNA isolated from cell nuclei purified from Mrd1p-GFP cells was analyzed by northern hybridization. The probes used were as follows: lane 1, probe 1; lane 2, probe 2. (**B**) Western blot analyses of Nop1p and CPY in extracts from total cells (T) or from purified nuclei (N). (**C**) Western blot analyses of *GAL::3HA-NOB1*/*MRD1-GFP*, grown in YPG (gal) or YPD (glu) for 15 h. (**D**) Northern hybridization using probe 2 of total RNA from wild-type (Mrd1p) and *GAL::3HA-NOB1*/*MRD1-GFP* cells, grown in YPG (gal) or YPD (glu). The 20S pre-rRNA is shown. (**E**) Northern hybridizations using probe 1 of total RNA isolated from *MRD1-GFP*, *GAL::3HA-NOB1*/*MRD1-GFP* grown in YPG (gal) or YPD (glu).

Mrd1p associates early with the pre-rRNA and subsequently is needed for compaction of the pre-rRNA into the SSU processome

We analyzed the effect of Mrd1p-GFP and Mrd1p depletion on the cotranscriptional assembly of 90S preribosomal complexes in spreads of active ribosomal genes in the EM. Figure 5 shows representative genes from control, mutant and depleted cells. In Mrd1p cells, transcription, assembly of pre-90S ribosomal complexes and processing occurred as described (4,5). The 5′-ends of the growing 35S transcripts were first packaged into small 5′ terminal knobs, also called 5′ETS particles (small arrows, Figure 5A), which are thought to include U3 snoRNP interacting with its known binding sites in the 5′ ETS. Further compaction of small subunit rRNA into 90S preribosomes/SSU processomes (larger arrows, Figure 5A) occurred at the typical time point during transcription, and normal levels of cotranscriptional cleavage at A_2 were observed (bracketed region, left panel Figure 5A).

When Mrd1p was depleted, 5′ETS particles were well formed (Figure 5B small arrows), indicating that Mrd1p is not required for 5′ETS particle formation on the pre-rRNA. Even though 5′ETS particles were formed when Mrd1p was depleted, analysis of a large number of genes ($N = 75$) indicated that SSU processomes were not. In control nondepleted cells, essentially all rRNA genes displayed transcripts that compacted into SSU processomes ($N > 100$). This suggests that Mrd1p is needed for 5′ETS particles to coalesce into the large SSU processomes.

This conclusion is supported by results with the Mrd1p-GFP protein, which also interfered with cotranscriptional assembly of the growing 35S pre-rRNA into SSU processomes (Figure 5C and D). The majority of genes showed long uncleaved transcripts with few or no 5′-terminal RNP particles (Figure 5C). Occasionally, some transcripts near the 3′-end of the genes formed 5′ETS particles (Figure 5C, small arrows), but the majority were not incorporated into typical structures. The EM results show that formation of 5′ETS particles on the 35S pre-rRNA was either partially abrogated or disturbed by Mrd1p-GFP, even more so than when Mrd1p was depleted. Combined, the results for Mrd1p-GFP and depletion of Mrd1p strongly suggest that Mrd1p-GFP binds early to the pre-rRNA, within the 5′ETS, and that the GFP moiety interferes with timely formation of the 5′ETS particle.

No genes with the normal cotranscriptional cleavage pattern were seen in the Mrd1p-GFP strain (Figure 5C and D) or the depleted strain (Figure 5B). Since small amounts of 20S pre-rRNA and 18S rRNA were still made in the presence of Mrd1p-GFP, this suggests that SSU processome formation and required cleavages are delayed until after transcription in those cases. In a number of genes in cells expressing Mrd1p-GFP, aberrant cotranscriptional cleavages were observed (Figure 5D). Although this unusual cleavage mapped to the general region of ITS1, as does normal cleavage, it had two features never seen in normal cotranscriptional cleavage at the A_2 site (4). First, it occurred without prior formation of either visible 5′ETS particles or visible SSU processomes, and second, it occurred on transcripts attached to polymerases that had transcribed only into ITS1, which is more upstream than is seen for normal A_2 cleavage. That is, normal A_2 cleavage requires transcription of RNA downstream of the A_2 cleavage site, including transcription through 5.8S rRNA and into ITS2 (Y.N. Osheim and A.L. Beyer, unpublished data). This unusual cotranscriptional cleavage seen in cells expressing Mrd1p-GFP is likely to represent the event resulting in the 22.5S rRNA. It is unlikely to represent cleavage at A_3 to generate 23S rRNA because A_3 cleavage requires the presence of the 3′ETS (43) and is not thought to occur cotranscriptionally (4).

Although the two examples shown for the Mrd1–GFP strain (Figure 5C and D) display transcripts that are either mainly cleaved or not cleaved, other genes showed a mixed population of transcripts on the same gene, with some cleaved, others not, and rarely with large SSU processome-like particles. We conclude from the EM analyses that in the presence of Mrd1p-GFP, the aberrant processing that results in the 22.5S rRNA described above appears to be at least partly cotranscriptional.

90S preribosomal complex components are required for the Mrd1p-GFP induced aberrant processing of pre-rRNA

The EM data showed that both depletion of Mrd1p and the presence of Mrd1p-GFP interfered with normal SSU processome formation (Figure 5). In contrast, while depletion of Mrd1p did not affect visible 5′ETS particle formation on pre-rRNA, EM showed that the 5′ETS particles formed less efficiently when Mrd1p-GFP was present. This might mean that U3 snoRNP was less efficiently recruited to or less stably associated with the nascent pre-rRNA, since U3 snoRNA is required for 5′ETS particle formation (4,5). Thus, we examined the association of U3 snoRNA with Mrd1p-GFP and the distribution of U3 snoRNP in sucrose gradients. Immunoprecipitation showed that U3 snoRNA is associated with Mrd1p-GFP (Figure 6B, IP). In wild-type cells, U3 snoRNP was mostly associated with 80–90S complexes (Figure 6A), with little free U3 snoRNP at the top of the gradient (about 17% of the hybridization signal in fractions 1–7). In the presence of Mrd1p-GFP, there was an increase in free U3 snoRNP with a corresponding decrease of U3 snoRNP in the 80–90S fractions (about 29% of the U3 snoRNA signal in fractions 1–7). The distribution of U14 snoRNA followed the same pattern (Figure 6A, a shift from about 39% to about 51% signal in fraction 1–7). Even if a shift of snoRNPs away from large pre-rRNA complexes is in line with a disturbed formation of 5′ ETS particles and SSU processomes, the considerable amount of snoRNPs in 80–90S complexes was higher than expected considering the dramatic effect of Mrd1p-GFP on formation of particles as displayed by EM. The discrepancy between the EM and gradient results could indicate that a suboptimally assembled preribosomal complex could be sensitive to methodological differences, in one case (Miller spreads) falling apart and in another (sucrose gradients) staying together. Alternatively, or in addition, this could reflect that stable U3 snoRNP association with pre-rRNA was delayed and not visible on nascent pre-rRNA. Since we observed that 35S

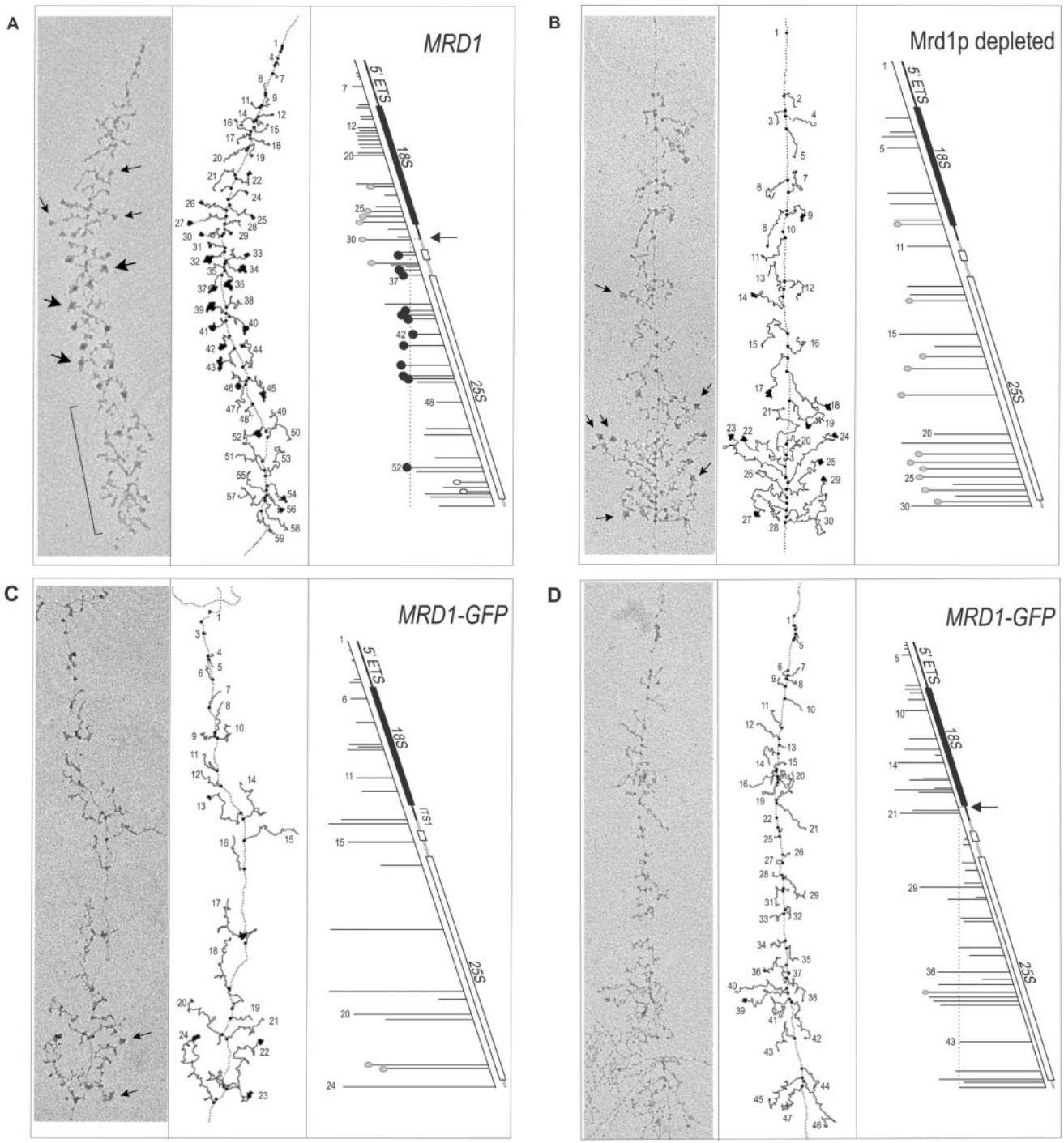

Figure 5. Mrd1p-GFP disturbs the cotranscriptional assembly of 90S preribosomal complexes. (**A**) Representative rRNA gene from control cells (Mrd1p) and an interpretive tracing of the gene, with small arrows indicating examples of small terminal knobs (thought to contain U3 snoRNP), and larger arrows indicating examples of SSU processomes. Bracketed region indicates cleaved transcript region. A transcript map of the gene is shown on the right. Transcripts are linearized and shown at the appropriate position along the gene. The gene is drawn on a slope so that the transcript sequences are approximately aligned in sequence, with 5′-termini to the left. Small (gray) and large (black) terminal particles are shown. For reference, the dotted line extrapolates to the site of A_2 cleavage, which is indicated by an arrow on the gene map. (**B**) The rRNA gene from cells in which Mrd1p was depleted for 20 h. Formation of 5′ particles (arrows) occurred, but SSU processomes were not formed. (**C**) The rRNA gene from Mrd1p-GFP cells showing little cotranscriptional A_2 cleavage of transcripts. (**D**) The rRNA gene from Mrd1p-GFP cells showing an unusual type of cotranscriptional cleavage. For reference, dotted line and arrow in the panel indicate the approximate position of the 3′-ends in the 22.5S rRNA (see text).

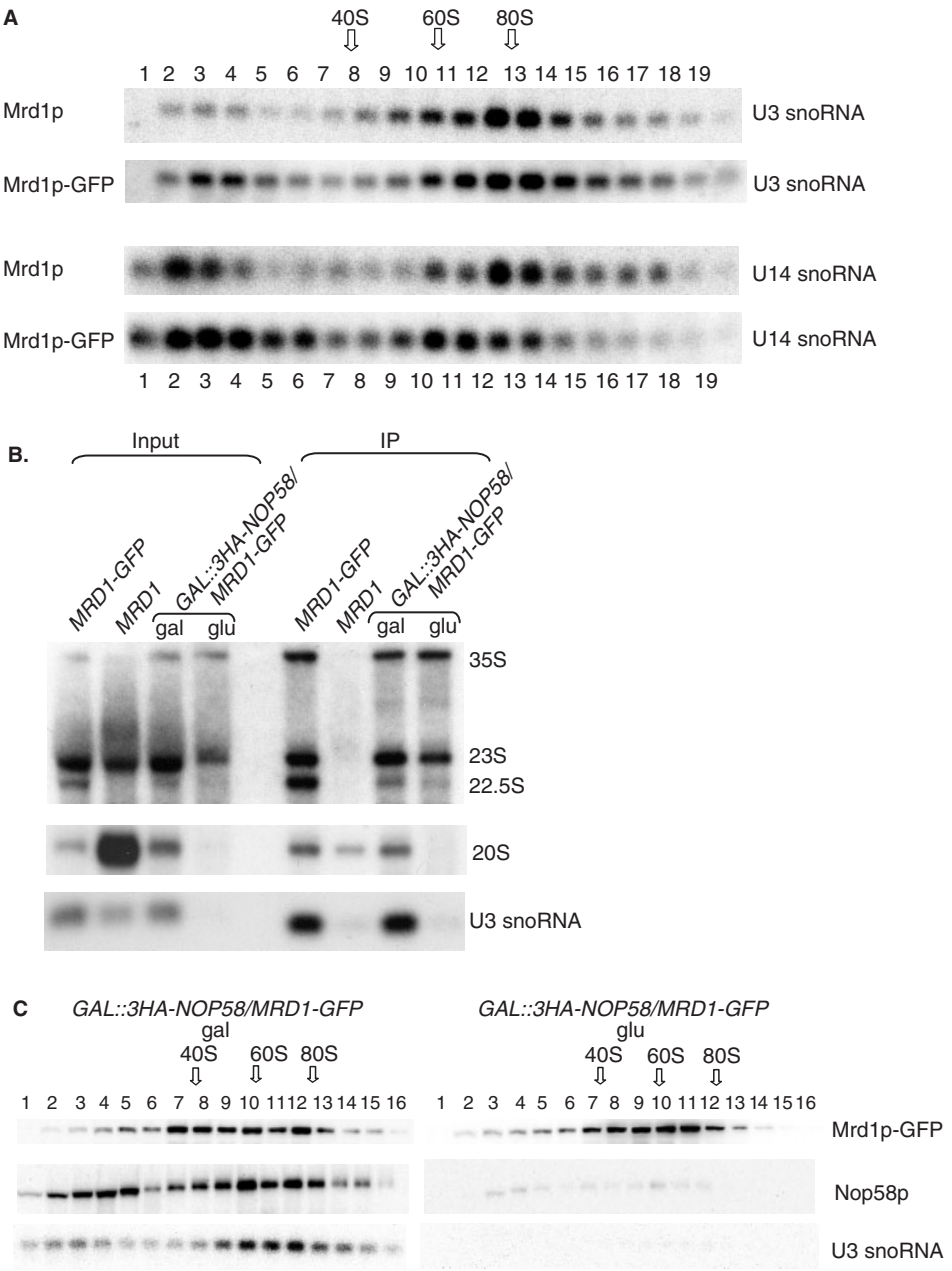

Figure 6. Mrd1p-GFP is compatible with the presence of U3 and U14 snoRNAs in 90S preribosomal complexes and U3 snoRNP is required for induction of the aberrant 22.5S rRNA, but not for Mrd1p-GFP association with 35S pre-rRNA and 23S rRNA. (**A**) Northern hybridizations using U3 or U14 snoRNA probes. Extracts from wt (Mrd1p) or Mrd1p-GFP were subjected to sucrose gradient centrifugation. RNA was extracted from each fraction and separated in 1.2% agarose/formaldehyde gels. The positions of 40S, 60S and 80S are indicated as determined from methylene blue staining of RNA in each fraction. (**B**) Extracts from cells with Mrd1p-GFP and Mrd1p grown in YPD and *GAL::3HA-NOP58/MRD1-GFP* grown in YPG (gal) or YPD (glu) for 16 h were immunoprecipitated with anti-GFP antibodies. RNA in the extracts (Input, 1/30 of total extract) and coimmunoprecipitated RNA (IP) was size separated on a 1.5% agarose gel and probed with probe 1, probe 2 and U3 probe. (**C**) Distribution of Mrd1p-GFP, 3HA-Nop58p and U3 snoRNA in 10–50% sucrose gradients. Extracts from *GAL::3HA-NOP58/MRD1-GFP* cells grown in YPG (gal) or YPD (glu) for 17 h were analyzed by western blotting or northern blotting with the U3 probe. The positions of 40S, 60S and 80S are indicated.

pre-rRNA accumulated extensively in the presence of Mrd1p-GFP (Figure 3A), it is possible that once U3 snoRNP was incorporated in a preribosomal complex, it remained there for an extended time period. It should also be noted that it is possible that the observed redistribution of the snoRNPs in sucrose gradients reflects slower growth of the Mrd1p-GFP containing cells, since growth rate influences snoRNP incorporation into 90S preribosomal complexes (44).

To further investigate the relationship between the aberrant processing induced by Mrd1p-GFP and its effect on 5′ETS particle formation, we constructed a Mrd1p-GFP strain with 3HA-Nop58p under the control of a galactose inducible GAL1 promotor. Depletion of Nop58p

destabilizes all C/D box snoRNPs, including U3 snoRNP (45). When U3 snoRNA was substantially depleted in glucose medium (by about 90%) (Figure 6B, compare Input, gal and glu), 20S and 22.5S rRNA were substantially reduced, while 35S pre-rRNA and 23S rRNA were still efficiently produced (Figure 6B, Input, glu). Coimmunoprecipitation showed that in the presence of U3 snoRNA, Mrd1p-GFP was associated with 35S and 20S pre-rRNA and with 23S and 22.5S rRNA (Figure 6B, IP, gal). When U3 snoRNA was depleted, Mrd1p-GFP was still associated with 35S pre-rRNA and 23S rRNA. Consistent with these data, Mrd1p-GFP was associated with large molecular complexes in the 80–90S region when Nop58p and U3 snoRNA were efficiently depleted (Figure 6C, glu). These results indicate that box C/D snoRNPs are not required for the association of Mrd1p-GFP with 35S pre-rRNA, but that Nop58p or one of its snoRNPs, possibly U3 snoRNP, is required for Mrd1p-GFP induction of the aberrant processing.

We asked if the aberrant processing, producing the 22.5S rRNA, was dependent on further components specific to the 90S preribosomal complex. Since Mrd1p-GFP could influence the association of U3 snoRNP with 35S pre-rRNA (Figures 5 and 6A), we focused on components within the 90S preribosomal complex involved in U3 snoRNA–pre-rRNA base pairing, Mpp10p (21,46) and Pwp2p (20) and also on Utp4p, classified as a t-Utp (22). The latter subcomplex is believed to assemble onto the 35S pre-rRNA very early and to be required for the subsequent assembly of other 90S preribosomal components (19).

We constructed strains with Mpp10p, Pwp2p and Utp4p under the control of a GAL1 promotor and an N-terminal 3HA tag in the Mrd1p-GFP background. Depletion of any one of the three 90S preribosomal complex components resulted in inhibition of cell growth (data not shown). Analysis of the pre-rRNA processing showed that depletion of Pwp2p, Mpp10p or Utp4p in all cases resulted in loss or a large decrease of the 22.5S rRNA (Figure 7A, glu lanes), supporting the conclusion that the 90S preribosomal complex is required for Mrd1p-GFP induction of the events that produced the 22.5S rRNA. Depletion of Pwp2p or Utp4p in this context also decreased the amount of other rRNA processing intermediates, consistent with the inhibition of cell growth and with Utp4p being important for efficient transcription of rRNA (22).

We conclude that known components required for correct assembly of 90S preribosomal complexes are also required for the Mrd1p-GFP-induced aberrant processing. This strongly indicates that the 22.5S rRNA is produced in the context of the 90S preribosomal complex. Furthermore, the combined results of EM and genetic depletion experiments suggest that the U3 snoRNP can associate with the 5′ part of the nascent pre-rRNA in the presence of Mrd1p-GFP, as seen by the requirement for U3 snoRNP/processome factors to generate the aberrant 22.5S processing which, at least in a fraction of transcripts, is visible in EM and hence cotranscriptional. This association of U3 snoRNP with pre-rRNA was however disturbed as seen by the large reduction in the number of 5′ETS particles in EM.

Pwp2p and Mpp10p functionally interact with Mrd1p-GFP

When the *PWP2* and *MPP10* genes were expressed from the GAL1 promoter in the Mrd1p-GFP background, we detected specific genetic interactions between Mrd1p-GFP and both Pwp2p and Mpp10p. No or very minor interaction was observed between Mrd1p-GFP and Utp4p, expressed from the GAL1 promoter.

First, processing of 35S pre-rRNA was influenced. The effect of Pwp2p was the most significant. Quantification showed a drastic decrease in the production of 22.5S rRNA (Figure 7A, gal lane). In addition, compared to *MRD1-GFP*, the 20S/23S rRNA ratio increased (Figure 7B, gal lane). GAL1-directed expression of Mpp10p increased the 22.5S/23S rRNA ratio slightly (Figure 7A, gal lane), while the 20S/23S rRNA ratio decreased (Figure 7B, gal lane). For Utp4p, GAL1-directed expression did not influence the relative amount of 22.5S rRNA (Figure 7A, gal lane), but the 20S/23S ratio increased as for Pwp2p (Figure 7B, gal lane). These effects were not due to decreased amounts of Mrd1p-GFP expression in the strains (data not shown).

To exclude the possibility of second site suppressors, strain PLY340 (*GAL::3HA-PWP2/MRD1-GFP*), was crossed to wt (*PWP2/MRD1*). All ascusspore-derived colonies with the *MRD1-GFP/PWP2* genotype had the same growth rate as PLY129 and produced the aberrant 22.5S rRNA (data not shown), thus eliminating the possibility that the loss of the aberrant processing in the cells with GAL1-directed expression of Pwp2p was due to mutations affecting the *MRD1-GFP* gene.

Second, GAL1-directed expression of Pwp2p improved cell growth in the Mrd1p-GFP strain background (Figure 7C). The generation time was ~4 h compared to 5 h for the Mrd1p-GFP strain. This was specific for the *MRD1-GFP* genotype, since GAL1-directed expression of Pwp2p in the wild-type background did not influence cell growth (data not shown). GAL1-directed expression of Mpp10p resulted in a reduction in cell growth, ~7 h generation time (Figure 7C), while GAL1-directed expression of Utp4p did not influence growth of cells containing Mrd1p-GFP (data not shown). Together, these results show that Pwp2p specifically suppressed the cleavage defects induced by Mrd1p-GFP, while Mpp10p in the presence of Mrd1p-GFP negatively influenced the A_0–A_2 cleavages. It is possible that the combined effect described above of decreased 22.5S rRNA synthesis and a relative increase in 20S pre-rRNA synthesis was involved in the higher growth rate in the case of GAL1-directed expression of Pwp2p. Similarly, a relative decrease in 20S pre-rRNA and a slight increase in synthesis of 22.5S rRNA could be involved in slower growth in the case of GAL1-directed expression of Mpp10p. In the case of GAL1-directed expression of Utp4p, a relative increase in 20S pre-rRNA synthesis, but unchanged amounts of 22.5S rRNA did not influence growth.

Third, EM analyses of rRNA genes from cells in which Pwp2p was expressed from the GAL1 promoter in the

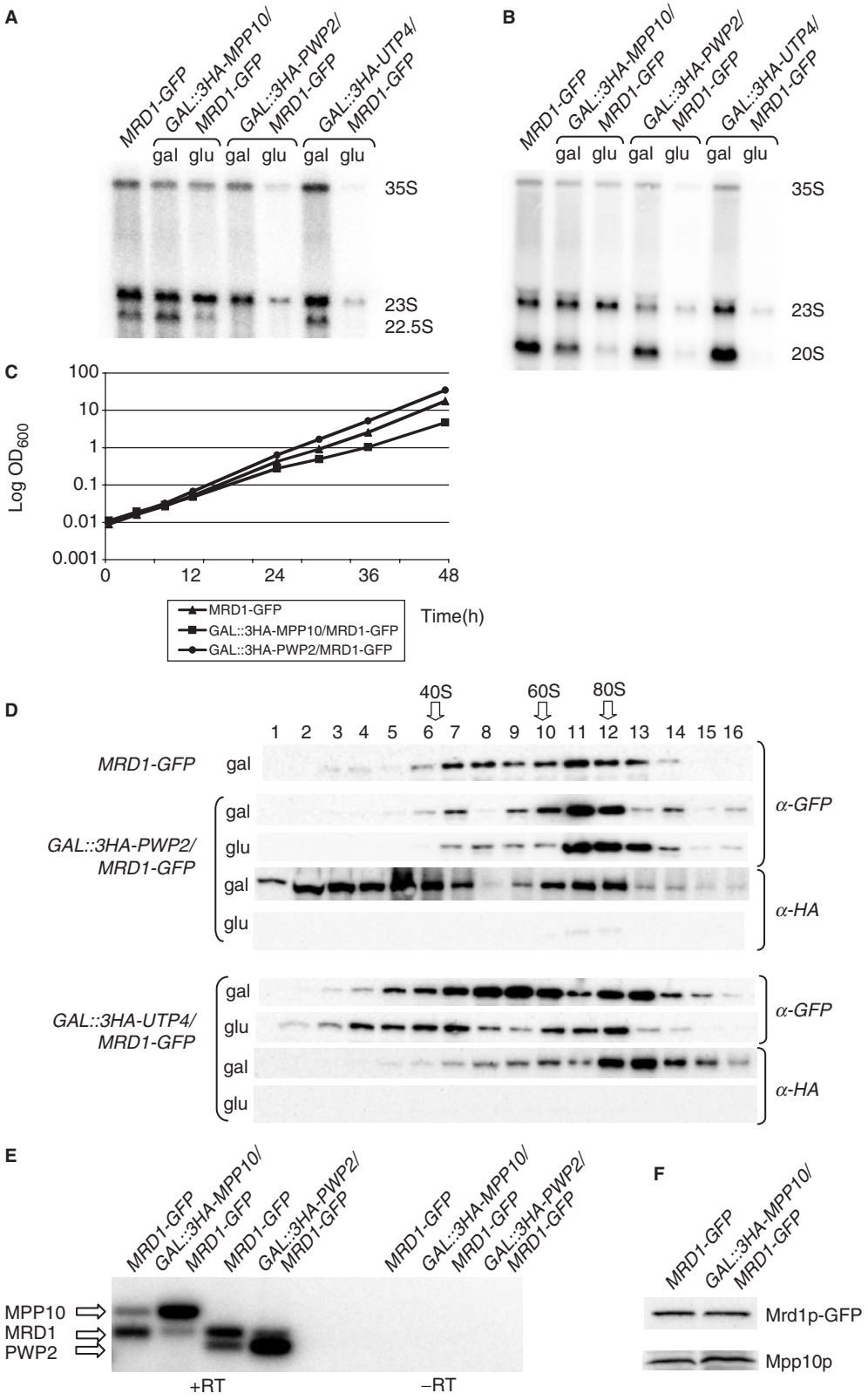

Figure 7. Pwp2p and Mpp10p influence the function of Mrd1p-GFP. (**A**) Northern hybridization using probe 1. Total RNA was extracted from Mrd1p-GFP cells and from cells with *GAL::3HA-MPP10/MRD1-GFP*, *GAL::3HA-PWP2/MRD1-GFP* and *GAL::3HA-UTP4/MRD1-GFP* grown in YPG (gal) or YPD (glu). The positions of pre-rRNA species are indicated to the right. The ratio between the hybridization signals for 22.5S and 23S were: 0.6 for MRD-GFP, 0.8 for MPP10 (gal), 0.2 for PWP2 (gal) and 0.6 for UTP4 (gal). (**B**) Northern hybridization using probe 2. RNA was extracted from cells as in (A). The ratio between the hybridization signals for 20S and 23S were:1.3 for MRD-GFP, 0.9 for MPP10 (gal), 1.7 for PWP2 (gal) and 1.6 for UTP4 (gal). (**C**) Comparison of the growth rate of *MRD1-GFP, GAL::3HA-MPP10/MRD1-GFP* and

Mrd1p-GFP background showed a definite increase in formation of the SSU processomes on nascent transcripts as compared to the Mrd1p-GFP strain, though many genes still showed slowed or abnormal cotranscriptional processing (data not shown).

Fourthy, GAL1-directed expression of Pwp2p also influenced the physical properties of 90S preribosomal complexes containing Mrd1p-GFP. Sucrose gradient analysis showed that Mrd1p-GFP was present in 80–90S preribosomal complexes both when Pwp2p was depleted and when expressed from the GAL1 promoter (Figure 7D). However, in both instances Mrd1p-GFP accumulated in 80–90S preribosomal complexes, compared to cells that expressed Pwp2p at endogenous levels (Figure 7D, compare Mrd1p-GFP distribution in *MRD1-GFP* with *GAL::3HA-PWP2/MRD1-GFP* gal and glu). This suggests a change in the structure and/or composition of the Mrd1p-GFP containing 90S preribosomal complexes. In addition, we observed that GAL1-directed expression of Pwp2p in the presence of Mrd1p-GFP further decreased the association of U3 snoRNP with 90S preribosomal complexes. 15–20% of the U3 snoRNA present in the 80–90S region in Mrd1p-GFP cells shifted towards the top of the gradient in cells expressing Pwp2p from the GAL1 promoter (data not shown).

The accumulation of Mrd1p-GFP in 80–90S complexes was specific for Pwp2p. GAL1-directed expression of Utp4p did not change the distribution of Mrd1p-GFP (Figure 7D). However, depletion of Utp4p resulted in a shift of part of the Mrd1p-GFP to lower fractions (compare *GAL::3HA-UTP4/MRD1-GFP* gal and glu in Figure 7D). A substantial part of Mrd1p-GFP remained in the 80–90S region. This would indicate that in contrast to many other ribosomal biogenesis factors, Mrd1p-GFP is not dependent on t-Utps for assembly onto the pre-rRNA (19).

The genetic interactions of Mrd1p-GFP with Pwp2p and with Mpp10p could be due to a changed balance between Mrd1p-GFP and these two proteins when expression was directed from the GAL1 promoter. This possibility was supported by the demonstration that the relative mRNA levels changed as a result of GAL1-directed expression (Figure 7E). Quantification showed that the ratio of Mrd1p-GFP:Mpp10p mRNA changed from 2.8 to 0.2 and the ratio of Mrd1p-GFP:Pwp2p mRNA changed from 1.6 to 0.2. Western blot analysis indicated that there was also a relative increase at the protein level for Mpp10p, though not as dramatic as the mRNA level (Figure 7F). Quantification showed that in relation to the Mrd1p-GFP amounts (PLY339: PLY129 ratio of 1), Mpp10p was slightly increased in PLY339 (PLY339:PLY129 ratio of 1.4). It is also possible that the presence of the GFP tag on Mrd1p and a 3HA-tag on Mpp10p and Pwp2p contributed to the functional interactions.

In summary, Pwp2p and Mpp10p exhibited specific genetic interactions with Mrd1p-GFP. These data indicate that both Pwp2p and Mpp10p functionally and possibly physically interact with Mrd1p in the context of the 90S preribosomal complex.

DISCUSSION

The 90S preribosomal complexes were first identified by sucrose gradient analysis (3). Extensive biochemical purifications, using affinity tagged proteins, have identified U3 snoRNA and a large number of proteins as components of the 90S preribosomal complex (5–7,18,47). In these purifications, several smaller complexes with partially overlapping components have been found, indicating the existence of subcomplexes within the 90S preribosomal complex and possibly that some components interact transiently with the complex. In addition, analyses of individual proteins and snoRNAs have shown that more components are likely to be part of the 90S preribosomal complex (9,46). The 90S preribosomal complex is dynamic during assembly and subsequent processing steps. This is reflected in EM of active rDNA genes, where different structures are visible along the partially unfolded 5′ part of the 35S pre-rRNA, eventually making up a compact structure encompassing the entire 18S rRNA part of the nascent transcript (4). Biochemical analyses have also shown that several subcomplexes associate with the 35S pre-rRNA in defined steps (19,22). In spite of these data, neither the *in vivo* composition and structure of the 90S preribosomal complex are known nor is the function of the individual components of the 90S preribosomal complex.

Mrd1p is part of the 90S preribosomal complex

Our results show that Mrd1p is part of the 90S preribosomal complex. This is in agreement with the recent identification of Mrd1p in some of the biochemically purified 90S preribosomal subcomplexes (10,47). Mrd1p is recruited to the 5′ part of the 35S pre-rRNA and is incorporated into 90S preribosomal complexes, even when U3 snoRNA, Pwp2p and Utp4p are depleted, suggesting that the association of Mrd1p with 35S pre-RNA is independent of these components. Our EM data show that the 5′ ETS particles form in the absence of Mrd1p. Since formation of the 5′ETS particles requires U3 snoRNA (4), this implies that U3 snoRNA directly or indirectly performs

GAL::3HA-PWP2/MRD1-GFP cells grown in YPG media for the time indicated. Cells were kept in exponential growth throughout the experiment by dilution in prewarmed medium. (**D**) Western blot analyses of Mrd1p-GFP, 3HA-Pwp2p and 3HA-Utp4p in fractions from sucrose gradients of cells containing *MRD1-GFP*, *GAL::3HA-PWP2/MRD1-GFP* and *GAL::3HA-UTP4/MRD1-GFP*. Cells were grown in YPG (gal) or YPD (glu) for 16 h. The positions of 40S, 60S and 80S are indicated. (**E**) Relative mRNA levels measured by RT–PCR. RNA was extracted from cells grown in galactose medium. These cells contained either the *MRD1-GFP* gene and all other genes expressed from their wild-type promoters (*MRD1-GFP*), or the MPP10 gene expressed from the GAL1 promoter and all other genes, including *MRD1-GFP* expressed from their wild-type promoters (*GAL::3HA-MPP10/MRD1-GFP*), or the PWP2 gene expressed from the GAL1 promoter and all other genes, including *MRD1-GFP* expressed from their wild-type promoters (*GAL::3HA-PWP2/MRD1-GFP*). PCR products corresponding to the different mRNAs are indicated. (**F**) Western blot of Mrd1p-GFP and Mpp10p in PLY129 and PLY339. The strains were grown in galactose medium. Proteins were extracted from the same number of cells and analyzed by western blotting, using an anti-GFP antibody and anti-Mpp10p antibodies.

this function in the absence of Mrd1p. Even though 5′ETS particles can form without Mrd1p, the finding that the GFP domain in Mrd1p-GFP hinders normal formation of the 5′ETS particles suggests that Mrd1p is associated with the transcript early during transcription, before U3 snoRNP is involved in 5′ETS particle formation.

The association of Mrd1p with the pre-rRNA is probably also largely independent of t-Utps (Figure 7D), but is lost when RNA polymerase I transcription is arrested (Figure 2B), indicating that pre-rRNA is necessary and sufficient for Mrd1p incorporation into preribosomal complexes. Together, our data thus suggest that Mrd1p is assembled early into the 90S preribosomal complex. Other components such as Rrp5 and the UTP-C components Utp22p and Rrp7p would then be incorporated later (19). We have however not investigated the relationship between Mrd1p and these components.

The combined data for Mrd1p-GFP and for Mrd1p depletion demonstrate that Mrd1p is required for compaction of the pre-18S rRNA into large, SSU processome particles as observed in the EM (Figure 5). Lack of Mrd1p prevents or drastically destabilizes such large particles and the extra GFP domain perturbs the structure and function of the particle. Our data therefore show that Mrd1p is essential for compaction of the pre-rRNA. We can furthermore coimmunoprecipitate Mrd1p-GFP with 35S pre-rRNA, 23S and 22.5S rRNA (Figure 6B), which all contain the intact A_0–A_2 cleavage sites. We cannot rule out that Mrd1p must dissociate before cleavages can occur. However, considering that Mrd1p-GFP is also associated with 20S pre-rRNA (Figure 6B), it appears more likely that Mrd1p must be present to organize conformations required for cleavages. The fact that Mrd1p-GFP at least to some extent remains with the 20S pre-rRNA could explain why we detected low levels of Mrd1p-GFP in the nucleoplasm, outside the nucleolus. As yet, we do not know where Mrd1p binds to the 35S pre-rRNA. However, Mrd1p is highly conserved in eukaryotes and we have previously shown that the corresponding protein in *Chironomus tentans*, RBD1, binds both to the 5′ETS and the ITS1 and ITS2 (33). If this is also the case for Mrd1p, this is consistent with the possibility that Mrd1p, with its multiple RBDs, might help guide the compaction by binding to sequences present at both ends of the pre-rRNA that is present in the SSU processome, bringing the A_1 site in the 5′ETS into proximity with the A_2 cleavage site in ITS1.

Esf2p, a protein believed to interact transiently with the SSU processome, is associated with the 5′ETS and is required for A_0–A_2 cleavages (48). Esf2p is important for release of U3 snoRNP from the 90S preribosomes, and the findings that Esf2p copurifies with Pwp2p and Mpp10p colocalizes with 90S preribosomal complexes on gradients (48), and acts as a binding partner and cofactor for the Dbp8p helicase (49), suggest that Esf2p may be directly involved in 90S preribosome dynamics. It is interesting to compare effects of Mrd1p depletion to effects of Esf2p depletion (48), since both of these situations allow U3 snoRNP incorporation into 80–90S complexes and both allow formation of 5′ETS particles as visualized by EM. The difference in the EM results is that in Esf2p-deficient cells, the assembly can progress beyond the 5′ETS particle stage to the stage of transcript compaction into a loose or pre-SSU processome (48). RNP assembly appears to halt at this stage in the absence of Esf2p, prior to formation of tight SSU processomes, which are the substrate for A_2 cleavage (4). The 5′ETS particles in Mrd1p-deficient cells show no evidence of compaction into loose or normal SSU processomes, though they sometimes appear slightly larger than normal. These results indicate that Mrd1p but not Esf2p is required for transcript compaction and formation of the larger particles.

In the Mrd1p-GFP strain, fewer 5′ETS particles are formed and formation is delayed in the few that form. Many genes exhibit long transcripts with no particles while other genes exhibit aberrant cleavage. This is consistent with the GFP moiety hindering timely 5′ETS particle formation, though other results indicate that preribosomal particles eventually form on some transcripts. That is, although the transcripts in the Mrd1p-GFP strain initially appear more abnormal than those in either the Esf2p-depleted or Mrd1p-depleted cells, some of these transcripts are eventually processed to 20S pre-rRNA while those in the depletion strains are not.

Although depletion of many individual 90S preribosomal complex components impairs cleavage at the A_0–A_2 sites, it appears that the U3 snoRNP, Pwp2 and Mpp10 subcomplexes are located close to the A_0–A_2 cleavage sites in the 90S preribosomal complex. Our data do not allow us to draw precise conclusions about the location of Mrd1p, but the functional interactions between Mrd1p-GFP and the U3 snoRNP, Pwp2 and Mpp10 subcomplexes suggest that Mrd1p is important for establishing productive structures within the 90S preribosomal complex. It is possible from our data that Mrd1p is physically located close to the U3 snoRNP, Pwp2 and Mpp10 subcomplexes.

Mrd1p influences the structure of a dynamic 90S preribosomal complex

Mrd1p-GFP supports correct processing at the A_0–A_2 sites. About one-fourth of the wild-type steady-state amount of 18S rRNA is made in the presence of Mrd1p-GFP (Figure 1D). To some extent, Mrd1p-GFP must therefore be compatible with correct binding of the U3 snoRNP, Pwp2 and Mpp10 subcomplexes. At the same time, it is striking that Mrd1p-GFP severely disturbs the function of the 90S preribosomal complex.

The correct processing that did take place was considerably delayed as seen from the accumulation of 35S pre-rRNA and from the chromatin spreads of the active rDNA genes. A delayed dissociation of U3 snoRNP was also indicated by the considerable presence of U3 snoRNP in 80–90S complexes in Mrd1p-GFP cells, and the increase in free U3 snoRNP when processing was partially rescued in the *GAL::3HA-PWP2/MRD1-GFP* suppressor strain. We did not detect degradation of the pre-rRNA, showing that Mrd1p-GFP did not induce breakdown of the pre-rRNA.

Mrd1p-GFP led to a significant decrease in cleavage at the A_0–A_2 sites, resulting in cleavage at the A_3 site and accumulation of 23S rRNA. This relative block in cleavage at the A_0–A_2 sites could be due to disturbance in U3 snoRNP associations in the 90S preribosomal complex, possibly due to a steric effect from the GFP moiety of Mrd1p-GFP. The EM data (Figure 5) showed in general a delayed and/or disturbed formation of 5′ ETS particles and failure of these particles to progress to compacted SSU processomes. The biochemical data combined with the EM data thus indicate that disturbed and/or less stable 90S preribosomal complexes are formed. EM analysis also showed that transcripts along the same gene could be independently affected by Mrd1p-GFP, suggesting that Mrd1p-GFP acts at the level of the individual 90S preribosomal complexes.

On some transcripts, Mrd1p-GFP induced changes in the 90S preribosomal complex that resulted in aberrant 3′-ends just downstream of the D-site in 35S pre-rRNA. The 22.5S rRNA was almost as common as 23S rRNA, indicating that the frequency by which these two latter events occurred was about the same. Aberrant processing intermediates called 22.5S have been described previously in strains depleted for proteins or with mutated versions of proteins implicated in preribosomal processing at the A_0–A_2 sites. These proteins include a putative RNA helicase (50), small and large ribosome subunit proteins (51,52), Lsm proteins (53) and one ribosome biogenesis factor needed both for 40S and 60S maturation (54). In all these instances, it was assumed that the 22.5S intermediate had been generated by cleavage at the D site, but the cleavage site was not mapped nor the location in the cell where the cleavage occurred. It is therefore possible that some or all of these 22.5S intermediates are identical to the 22.5S characterized in the Mrd1p-GFP strain. Since we detected a low amount of aberrant processing in wt cells (Figure 3C), it is conceivable that any mutation that affects preribosomal assembly/structure at this step can shift the equilibrium towards 22.5S rRNA production. Our data indicate that the aberrant events producing 22.5S rRNA take place within the 90S preribosomal complex, containing the U3 snoRNP, Pwp2 and Mpp10 subcomplexes. The 22.5S rRNA may represent multiple initial cleavage products, or alternatively, 3′-5′ exonucleolytic trimming of a downstream cleavage product. For example, the delayed or altered assembly of U3 snoRNP and other components onto transcripts in the presence of Mrd1p-GFP may expose several new cleavage sites somewhat downstream of the D site, or one new site whose 3′-end is subject to trimming. Combined, these data are consistent with the view that the 90S preribosomal complex is a highly dynamic structure in which Mrd1p influences the folding of the 35S pre-rRNA and the contacts that are present between the different components and the pre-rRNA necessary for correct cleavages in the 90S preribosomal complex. The fact that the presence of Mrd1p-GFP can lead to three different functional results for the 90S preribosomal complex suggests that the structure is flexible, where some structural states are consistent with correct binding of U3 snoRNP and cleavage at the A_0–A_2 sites and other states are not. Even though it is possible that Mrd1p is also involved in protein–protein interactions, our data in combination with the fact that Mrd1p contains five evolutionarily conserved RBDs, suggest that Mrd1p plays a role in folding of the pre-rRNA in the 90S preribosomal complex.

ACKNOWLEDGEMENTS

We thank Kerstin Bernholm for excellent technical assistance, S.J. Baserga for anti-Mpp10p antibodies, O. Gadal for the plasmid pUN100-DsRed-Nop1 and P.O. Ljungdahl for strains and plasmids. This work was supported by the Swedish Research Fund, Magnus Bergvalls Stiftelse and Carl Tryggers Stiftelse, and by NSF grant MCB-0448171 to A.L.B. Funding to pay the Open Access publication charges for this article was provided by Swedish Research Fund.

Conflict of interest statement. None declared.

REFERENCES

1. Venema,J. and Tollervey,D. (1999) Ribosome synthesis in *Saccharomyces cerevisiae*. *Annu. Rev. Genet*., **33**, 261–311.
2. Udem,S.R. and Warner,J.R. (1972) Ribosomal RNA synthesis in *Saccharomyces cerevisiae*. *J. Mol. Biol*., **65**, 227–242.
3. Trapman,J., Retél,J. and Planta,R.J. (1975) Ribosomal precursor particles from yeast. *Exp. Cell Res*., **90**, 95–104.
4. Osheim,Y.N., French,S.L., Keck,K.M., Champion,E.A., Spasov,K., Dragon,F., Baserga,S.J. and Beyer,A.L. (2004) Pre-18S ribosomal RNA is structurally compacted into the SSU processome prior to being cleaved from nascent transcripts in *Saccharomyces cerevisiae*. *Mol. Cell*, **16**, 943–954.
5. Dragon,F., Gallagher,J.E., Compagnone-Post,P.A., Mitchell,B.M., Porwancher,K.A., Wehner,K.A., Wormsley,S., Settlage,R.E., Shabanowitz,J., Osheim,Y. *et al.* (2002) A large nucleolar U3 ribonucleoprotein required for 18S ribosomal RNA biogenesis. *Nature*, **417**, 967–970.
6. Grandi,P., Rybin,V., Bassler,J., Petfalski,E., Strauss,D., Marzioch,M., Schafer,T., Kuster,B., Tschochner,H., Tollervey,D. *et al.* (2002) 90S pre-ribosomes include the 35S pre-rRNA, the U3 snoRNP, and 40S subunit processing factors but predominantly lack 60S synthesis factors. *Mol. Cell*, **10**, 105–115.
7. Bernstein,K.A., Gallagher,J.E.G., Mitchell,B.M., Granneman,S. and Baserga,S.J. (2004) The small-subunit processome is a ribosome assembly intermediate. *Eukaryot. Cell*, **3**, 1619–1626.
8. Bleichert,F., Granneman,S., Osheim,Y.N., Beyer,A.L. and Baserga,S.J. (2006) The PINc domain protein Utp24, a putative nuclease, is required for the early cleavage steps in 18S rRNA maturation. *Proc. Natl Acad. Sci. USA*, **103**, 9464–9469.
9. Kressler,D., Linder,P. and de La Cruz,J. (1999) Protein trans-acting factors involved in ribosome biogenesis in Saccharomyces cerevisiae. *Mol. Cell. Biol*., **19**, 7897–7912.
10. Thomson,E., Rappsilber,J. and Tollervey,D. (2007) Nop9 is an RNA binding protein present in pre-40S ribosomes and required for 18S rRNA synthesis in yeast. *RNA*, **13**, 2165–2174.
11. Tschochner,H. and Hurt,E. (2003) Pre-ribosomes on the road from the nucleolus to the cytoplasm. *Trends Cell Biol*., **13**, 255–263.
12. Kiss,T. (2002) Small nucleolar RNAs: an abundant group of noncoding RNAs with diverse cellular function. *Cell*, **109**, 148–148.
13. Fatica,A., Tollervey,D. and Dlaki,M. (2004) PIN domain of Nob1p is required for D-site cleavage in 20S pre-rRNA. *RNA*, **10**, 1698–1701.
14. Fatica,A., Oeffinger,M., Dlaki,M. and Tollervey,D. (2003) Nob1p is required for cleavage of the 3′ end of 18S rRNA. *Mol. Cell. Biol*., **23**, 1798–1807.
15. El Hage,A. and Tollervey,D. (2004) A surfeit of factors: why is ribosome assembly so much more complicated in eukaryotes than bacteria? *RNA Biol*., **1**, 10–15.

16. Veinot-Drebot,L.M., Singer,R.A. and Johnston,G.C. (1988) Rapid initial cleavage of pre-rRNA transcripts in yeast. *J. Mol. Biol.*, **199**, 107–113.
17. Grainger,R.M. and Maizels,N. (1980) *Dictyostelium* ribosomal RNA is processed during transcription. *Cell*, **20**, 619–623.
18. Krogan,N.J., Peng,W.T., Cagney,G., Robinson,M.D., Haw,R., Zhong,G., Guo,X., Zhang,X., Canadien,V., Richards,D.P. *et al.* (2004) High-definition macromolecular composition of yeast RNA-processing complexes. *Mol. Cell.*, **13**, 225–239.
19. Pérez-Fernández,J., Román,A., De Las Rivas,J., Bustelo,X.R. and Dosil,M. (2007) The 90S preribosome is a multimodular structure that is assembled trough a hierarchical mechanism. *Mol. Cell. Biol.*, **27**, 5414–5429.
20. Dosil,M. and Bustelo,X.R. (2004) Functional characterization of Pwp2p, a WD family protein essential for the assembly of the 90S pre-ribosomal particle. *J. Biol. Chem.*, **279**, 37385–37397.
21. Wehner,K.A., Gallagher,J.E. and Baserga,S.J. (2002) Components of an interdependent unit within the SSU processome regulate and mediate its activity. *Mol. Cell. Biol.*, **22**, 7258–7267.
22. Gallagher,J.E., Dunbar,D.A., Granneman,S., Mitchell,B.M., Osheim,Y.N., Beyer,A.L. and Baserga,S.J. (2004) RNA polymerase I transcription and pre-rRNA processing are linked by specific SSU processome components. *Genes Dev.*, **18**, 2506–2517.
23. Baudin-Baillieu,A., Tollervey,D., Cullin,C. and Lacroute,F. (1997) Functional analysis of Rrp7p, an essential yeast protein involved in pre-rRNA processing and ribosome assembly. *Mol. Cell. Biol.*, **17**, 5023–5032.
24. Rudra,D., Mallick,J., Zhao,Y. and Warner,J.R. (2007) Potential interface between ribosomal protein production and pre-rRNA processing. *Mol. Cell. Biol.*, **27**, 4815–4824.
25. Beltrame,M., Henry,Y. and Tollervey,D. (1994) Mutational analysis of an essential binding site for the U3 snoRNA in the 5′ external transcribed spacer of yeast pre-rRNA. *Nucleic Acids Res.*, **22**, 5139–5147.
26. Beltrame,M. and Tollervey,D. (1995) Base pairing between U3 and the pre-ribosomal RNA is required for 18S rRNA synthesis. *EMBO J.*, **14**, 4350–4356.
27. Hughes,J.M. and Ares,M. Jr. (1991) Depletion of U3 small nucleolar RNA inhibits cleavage in the 5′ external transcribed spacer of yeast pre-ribosomal RNA and impairs formation of 18S ribosomal RNA. *EMBO J.*, **10**, 4231–4239.
28. Hughes,J.M. (1996) Functional base-pairing interaction between highly conserved elements of U3 small nucleolar RNA and the small ribosomal subunit RNA. *J. Mol. Biol.*, **259**, 645–654.
29. Mereau,A., Fournier,R., Gregoire,A., Mougin,A., Fabrizio,P., Lührmann,R. and Branlant,C. (1997) An in vivo and in vitro structure-function analysis of the *Saccharomyces cerevisiae* U3A snoRNP: protein-RNA contacts and base-pair interaction with the pre-ribosomal RNA. *J. Mol. Biol.*, **273**, 552–571.
30. Sharma,K. and Tollervey,D. (1999) Base pairing between U3 small nucleolar RNA and the 5′ end of 18S rRNA is required for pre-rRNA processing. *Mol. Cell. Biol.*, **19**, 6012–6019.
31. Granneman,S. and Baserga,S.J. (2004) Ribosome biogenesis: of knobs and RNA processing. *Exp. Cell. Res.*, **296**, 43–50.
32. Jin,S-B., Zhao,J., Björk,P., Schmekel,K., Ljungdahl,P.O. and Wieslander,L. (2002) Mrd1p is required for processing of pre-rRNA and for maintenance of steady-state levels of 40S ribosomal subunits in yeast. *J. Biol. Chem.*, **277**, 18431–18439.
33. Björk,P., Bauren,G., Jin,S., Tong,Y.G., Bürglin,T.R., Hellman,U. and Wieslander,L. (2002) A novel conserved RNA-binding domain protein, RBD-1, is essential for ribosome biogenesis. *Mol. Biol. Cell*, **13**, 3683–3695.
34. De Gaudenzi,J., Frasch,A.C. and Clayton,C. (2005) RNA-binding domain proteins in kinetoplastids: a comparative analysis. *Eukaryot. Cell*, **4**, 2106–2114.
35. Longtine,M.S., McKenzie,A. III, Demarini,D.J., Shah,N.G., Wach,A., Brachat,A., Philippsen,P. and Pringle,J.R. (1998) Additional modules for versatile and economical PCR-based gene deletion and modification in *Saccharomyces cerevisiae*. *Yeast*, **14**, 953–961.
36. Gietz,D., St Jean,A., Woods,R.A. and Schiestl,R.H. (1992) Improved method for high efficiency transformation of intact yeast cells. *Nucleic Acids Res.*, **20**, 1425.
37. Elble,R. (1992) A simple and efficient procedure for transformation of yeasts. *BioTechniques*, **13**, 18–20.
38. Sambrook,J. and Russell,D.W. (2001) *Molecular Cloning: A Laboratory Manual*. Cold Spring Harbor Laboratory, Cold Spring Harbor, NY.
39. Aris,J.P. and Blobel,G. (1991) Isolation of yeast nuclei. *Methods Enzymol.*, **194**, 735–749.
40. Wise,J.A. (2004) Preparation and analysis of low molecular weight RNAs and small ribonucleoproteins. *Methods Enzymol.*, **194**, 405–415.
41. Dunbar,D.A., Wormsley,S., Agentis,T.M. and Baserga,S.J. (1997) Mpp10p, a U3 small nucleolar ribonucleoprotein component required for pre-18S rRNA processing in yeast. *Mol. Cell. Biol.*, **17**, 5803–5812.
42. Nogi,Y., Yano,R., Dodd,J., Carles,C. and Nomura,M. (1993) Gene *RRN4* in *Saccharomyces cerevisiae* encodes the A12.2 subunit of RNA polymerase I and is essential only at high temperatures. *Mol. Cell. Biol.*, **13**, 114–122.
43. Allmang,C. and Tollervey,D. (1998) The role of the 3′ external transcribed spacer in yeast pre-rRNA processing. *J. Mol. Biol.*, **278**, 67–78.
44. Kos,M. and Tollervey,D. (2005) The putative RNA helicase Dbp4p is required for release of the U14 snoRNA from preribosomes in *Saccharomyces cerevisiae*. *Mol. Cell*, **20**, 53–64.
45. Lafontaine,D.L.J. and Tollervey,D. (1999) Nop58 is a common component of the box C + D snoRNPs that is required for snoRNA stability. *RNA*, **5**, 455–467.
46. Lee,S.J. and Baserga,S.J. (1999) Imp3p and Imp4p, two specific components of the U3 small nucleolar ribonucleoprotein that are essential for pre-18S rRNA processing. *Mol. Cell. Biol.*, **19**, 5441–5452.
47. Gavin,A.C., Aloy,P., Grandi,P., Krause,R., Boesche,M., Marzioch,M., Rau,C., Jensen,L.J., Bastuck,S., Dümplefeld,B. *et al.* (2006) Proteome survey reveals modularity of the yeast cell machinery. *Nature*, **440**, 631–636.
48. Hoang,T., Peng,W.-T., Vanrobays,E., Krogan,N., Hiley,S., Beyer,A.L., Osheim,Y.N., Greenblatt,J., Hughes,T.R. and Lafontaine,D.L. (2005) Esf2p, a U3-associated factor required for small-subunit processome assembly and compaction. *Mol. Cell. Biol.*, **25**, 5523–5534.
49. Granneman,S., Lin,C., Champion,E.A., Nandineni,M.R., Zorca,C. and Baserga,S.J. (2006) The nucleolar protein Esf2 interacts directly with the DexD/H box RNA helicase Dbp8 to stimulate ATP hydrolysis. *Nucleic Acids Res.*, **34**, 3189–3199.
50. Colley,A., Beggs,J.D., Tollervey,D. and Lafontaine,D.L.J. (2000) Dhr1p, a putative DEAH-Box RNA helicase, is associated with the box C + D snoRNP U3. *Mol. Cell. Biol.*, **20**, 7238–7246.
51. Ferreira-Cerca,S., Pöll,G., Gleizes,P.-E., Tschochner,H. and Milkereit,P. (2005) Roles of eukaryotic ribosomal proteins in maturation and transport of pre-18S rRNA and ribosome function. *Mol. Cell*, **20**, 263–275.
52. Martín-Marcos,P., Hinnebusch,A.G. and Tamame,M. (2007) Ribosomal protein L33 is required for ribosome biogenesis, subunit joining and repression of *GCN4* translation. *Mol. Cell. Biol.*, **27**, 5968–5985.
53. Kufel,J., Allmang,C., Petfalski,E., Beggs,J. and Tollervey,D. (2003) Lsm proteins are required for normal processing and stability of ribosomal RNAs. *J. Biol. Chem.*, **278**, 2147–2156.
54. Oeffinger,M., Fatica,A., Rout,M.P. and Tollervey,D. (2007) Yeast Rrp14p is required for ribosomal subunit synthesis and for correct positioning of the mitotic spindle during mitosis. *Nucleic Acids Res.*, **35**, 1354–1366.